Chemical Engineering Journal 512 (2025) 162336

Contents lists available at ScienceDirect

Chemical Engineering Journal

journal homepage: www.elsevier.com/locate/cej

RiboJ-assisted non-repeated sgRNA arrays for enhanced CRISPR multiplex genome engineering in *Escherichia coli*

Seung-Gyun Woo [a,b,1], Seong Keun Kim [a,1], Tae Hyun Kim [a,c], Subeen Kim [a,d], Youshin Kim [a,d], Seung-Goo Lee [a,c,d,*], Dae-Hee Lee [a,c,d,e,*]

[a] Synthetic Biology Research Center and the K-Biofoundry, Korea Research Institute of Bioscience and Biotechnology (KRIBB), Daejeon 34141, Republic of Korea
[b] Department of Molecular Biosciences, University of Texas at Austin, Austin, TX 78712, USA
[c] Department of Biosystems and Bioengineering, KRIBB School of Biotechnology, University of Science and Technology (UST), Daejeon 34113, Republic of Korea
[d] Graduate School of Engineering Biology, Korea Advanced Institute of Science and Technology (KAIST), Daejeon 34141, Republic of Korea
[e] Department of Integrative Biotechnology, College of Biotechnology and Bioengineering, Sungkyunkwan University, Suwon-si, Gyeonggi-do 16419, Republic of Korea

ARTICLE INFO

Keywords:
Base Editing
Multiplex Genome Editing
RiboJ-Aided Multiplexed Base Editing (RAMBE)
Non-Repetitive RAMBE (NR-RAMBE)
Metabolic Engineering
Synthetic Biology

ABSTRACT

CRISPR-based systems have revolutionized genome editing by enabling precise and efficient genetic modifications. However, achieving multiplex genome editing remains challenging due to limitations in encoding, transcribing, and processing multiple single-guide RNAs (sgRNAs) in repetitive DNA arrays. In this study, we present the RiboJ-Aided Multiplexed Base Editing (RAMBE) system and its advanced iteration, the Non-Repetitive RAMBE (NR-RAMBE) system, designed for efficient and scalable multiplex genome engineering in *Escherichia coli*. The RAMBE system leverages RiboJ insulators to autonomously process sgRNA arrays, enhancing sgRNA maturation and enabling simultaneous multi-gene editing. We demonstrate editing of up to six endogenous genes in *E. coli* Nissle 1917 (EcN) in a single step, achieving high target-specific efficiencies of up to 100%, depending on the target and context. This multiplex editing enabled robust butyrate production and improved acetate utilization in engineered EcN strains. Building on this, the NR-RAMBE system incorporates diverse ribozymes and engineered non-repetitive sgRNA handles to minimize sequence repetition. This design reduced synthesis complexity and enabled simultaneous editing of six genomic loci with efficiencies comparable to those of the RAMBE system. The NR-RAMBE system broadens the scope of CRISPR multiplexing by allowing precise and scalable genome editing without labor-intensive sgRNA array assembly, paving the way for diverse large-scale genomic applications.

1. Introduction

Synthetic biology has transformed the design and engineering of biological systems, enabling remarkable advancements in microbial cell factories [1], cell-based therapies [2], living biomaterials [3], and whole-cell biosensors [4]. These applications heavily rely on precise genetic modifications to create or enhance specific functionalities. CRISPR-based systems have revolutionized genome engineering due to their exceptional programmability and efficiency [5–7]. The natural multiplexing capability of CRISPR–Cas systems, which encode multiple CRISPR arrays and express Cas proteins for spacer acquisition and array processing, highlights their potential for simultaneous multi-gene editing [8]. However, the widespread reliance on individual sgRNAs limits scalability and reduces the efficiency of advanced CRISPR applications, such as complex genome editing and transcriptional regulation [9].

To address these constraints, multiplexed strategies have been developed to enable simultaneous editing at multiple loci. These methods emulate the natural state of CRISPR systems by employing parallel expression of multiple sgRNAs or Cas proteins, enhancing modularity and scalability [9]. Recent developments have explored multiple strategies to encode, transcribe, and process sgRNA arrays more efficiently. One widely adopted approach encodes each sgRNA in an individual expression cassette with its own promoter and terminator. While this method has been successfully applied in yeast [10–12], plants [13,14], and mammalian cells [15–17], it becomes infeasible for larger sgRNA arrays due to structural complexity, reduced plasmid assembly

* Corresponding authors.
E-mail addresses: sglee@kribb.re.kr (S.-G. Lee), dhlee@kribb.re.kr (D.-H. Lee).
[1] These authors contributed equally to this work.

https://doi.org/10.1016/j.cej.2025.162336
Received 26 January 2025; Received in revised form 28 March 2025; Accepted 4 April 2025
Available online 7 April 2025

efficiency, and uneven sgRNA expression [18]. Another strategy encodes multiple sgRNAs in a single transcript, which can then be processed by native CRISPR–Cas systems such as Cas12a and Cas13a [19–23]. These Cas proteins possess intrinsic RNase activity, enabling them to efficiently process crRNA arrays. A third strategy incorporates external RNA cleavage sequences, including self-cleaving ribozymes and tRNA-processing systems, to generate multiple sgRNAs from a single transcript in systems lacking RNase activity [18,24–30]. This method improves sgRNA modularity and stoichiometry, facilitating multiplexed gene editing across various hosts, including microorganisms [18,24], plants [25], and mammalian cells [26]. In addition to arrayed sgRNA strategies, alternative approaches such as degenerate guide RNAs or guide RNAs incorporating universal bases have been developed to allow Cas9 and Cas12a to recognize and cleave polymorphic sequences [31].

Despite these advancements, achieving precise and scalable multiplex genome editing remains a significant technical challenge because current CRISPR-based approaches for multiplex genome editing typically rely on repetitive sgRNA arrays [5,32]. Repetitive DNA sequences within sgRNA arrays complicate synthesis and assembly, while increasing susceptibility to homologous recombination [33–35]. These repetitive sequences provide homologous regions that promote RecA-dependent or RecA-independent recombination and are prone to replication slippage during DNA replication, particularly on the lagging strand. Such events can lead to deletions, rearrangements, or loss of sgRNA cassettes, ultimately causing genetic instability [33,36,37]. Additionally, the co-expression of auxiliary processing enzymes, such as Cas endonucleases (e.g., Csy4, Cas6) [24,27,28], can introduce cytotoxic effects at high concentrations, further limiting the scalability of these methods [38]. These issues constrain the scalability of CRISPR technologies, especially in applications such as redirecting metabolic fluxes [32,37], performing large-scale genome rearrangements [39,40], and probing gene regulatory networks [41,42].

To overcome these challenges, we developed the RiboJ-Aided Multiplexed Base Editing (RAMBE) system, which leverages RiboJ—a self-cleaving ribozyme—to efficiently process sgRNA arrays and insulate genetic elements. This system enables precise and simultaneous editing of multiple genes from a single transcript. Building upon this platform, we introduced the Non-Repetitive RAMBE (NR-RAMBE) system, which incorporates diverse ribozymes and engineered non-repetitive sgRNA handles to eliminate the limitations of repetitive DNA sequences. To validate the utility of these systems, we focused on *Escherichia coli* Nissle 1917 (EcN), a well-studied probiotic strain known for its diagnostic and therapeutic potential [43,44]. EcN's resistance to genetic modifications poses a significant challenge for broader applications [45]. Using the RAMBE system, we achieved efficient and simultaneous multi-gene editing in EcN, leading to enhanced butyrate production and optimized acetate utilization. Furthermore, the NR-RAMBE system enabled the scalable and cost-effective assembly of non-repetitive sgRNA arrays, expanding the applicability of CRISPR multiplexing. These innovations address critical limitations in genome editing and provide a robust platform for transformative applications in synthetic biology, metabolic engineering, and therapeutic development [6,7,37,38,46].

2. Results and Discussion

2.1. Establishment of a RiboJ-aided base editing system

To enhance the processing efficiency of synthetic sgRNA arrays, we developed a RiboJ-aided base editing (BE) strategy. RiboJ acts as a genetic insulator by cleaving the 5′-untranslated region (UTR) of mRNA, reducing unintended *cis*-interactions and increasing transcript abundance [47]. Additionally, since *E. coli* promoters often generate multiple transcription start sites (TSS) [48], the use of RiboJ helps standardize sgRNA transcripts by removing heterogeneous 5′-UTRs, ensuring consistent sgRNA processing and activity. This feature makes RiboJ a powerful tool for applications requiring precise control of gene expression. Traditionally, hammerhead (HH) and hepatitis delta virus (HDV) ribozymes have been used for RNA cleavage [49,50]. These conventional self-cleaving ribozymes are mainly employed for precise RNA processing but often require sequence adaptation to the adjacent spacer region to ensure efficient cleavage [49]. This requirement can complicate construct design and potentially cause variability in processing efficiency depending on the spacer sequence. In contrast, RiboJ operates independently of spacer sequence context while providing both insulation and RNA processing capabilities [47]. Moreover, RiboJ's self-cleaving activity is autocatalytic and does not require any external inducer, enabling constitutive activity upon transcription. This dual functionality makes RiboJ particularly valuable for robust and scalable multiplex genome editing applications. Building on this, we further repurposed RiboJ as an RNA processing element for sgRNA maturation in this study. To directly compare the efficiency of RiboJ and HH ribozymes, we designed a fluorescent reporter system in which the BE system restored GFP expression by converting a silent start codon (ACG) to ATG. BE2 (rAPOBEC1-dCas9-UGI) and silent *gfp* were expressed under the P_{J23100} promoter, while HH-sgRNA or RiboJ-sgRNA were expressed under the P_{tet} promoter (Fig. S1A). BE efficiencies were quantified by measuring GFP fluorescence. RiboJ-sgRNA processing yielded fluorescence values significantly higher than HH-sgRNA, with the latter showing fluorescence levels 56 % lower under identical conditions (Fig. S1B). These results highlight RiboJ's superior sgRNA processing efficiency, making it a highly effective tool for BE system.

We constructed BE plasmids expressing cytidine deaminase fused to dCas9 (rAPOBEC1-dCas9-UGI) or nCas9 (rAPOBEC1-nCas9-UGI), along with a RiboJ-sgRNA cassette driven by the $P_{J23100/tetO}$ promoter. Upon anhydrotetracycline (aTc) induction, RiboJ efficiently cleaved upstream sequences, generating functional sgRNAs for base editing (Fig. 1A). This system was validated using sgRNAs targeting the endogenous *ldhA* gene in EcN. Expression of RiboJ-sgRNA with BE2 (rAPOBEC1-dCas9-UGI) or BE3 (rAPOBEC1-nCas9-UGI) proteins enabled C-to-T base conversions at position 4 (counting the TGG PAM at positions 21–23) of *ldhA* (Fig. 1B), increasing editing efficiencies from 0 % to 24 % for BE2 and from 16 % to 59 % for BE3 after multiple culture transfers (Fig. 1C). Given the higher efficiency of BE3, it was used for subsequent experiments. Next, we assessed the metabolic impact of *ldhA* inactivation by measuring lactate and pyruvate production. *ldhA* editing significantly reduced lactate levels while increasing pyruvate accumulation, confirming the expected metabolic shift (Fig. 1D, 1E). To further validate editing efficiency at the colony level, edited cell cultures were plated, and ten colonies per condition were sequenced. The sequencing results revealed inactivation frequency of 60 % for *ldhA* (Q18X) and 90 % for *ldhA* (Q250X). These values were consistent with the population-level editing efficiencies, which reached 59 % for Q18X and 100 % for Q250X, as confirmed by overlapping C/T peaks in Sanger sequencing data (Fig. 1F, 1G).

The general applicability of RiboJ-sgRNA processing was then evaluated by targeting additional endogenous genes in EcN, including *ldhA*, *adhE*, *frdA*, and *pta* (Fig. 1H). These genes encode enzymes involved in byproduct (lactate, ethanol, succinate, and acetate) formation from glucose metabolism in EcN, and their inactivation is hypothesized to increase intracellular acetyl-CoA levels, thereby enhancing production of acetyl-CoA-derived products. For each gene, two sgRNA designs were tested to optimize the C-to-T editing efficiency. Editing efficiencies for other targets were similarly high: up to 94 % for *adhE*, 94 % for *frdA*, and 98.7 % for *pta*. However, efficiency for *pta* decreased over successive culture transfers, likely due to growth disadvantages associated with *pta* knockout (Fig. 1F). By improving sgRNA processing and editing efficiency, the RiboJ-BE3 system demonstrated consistent performance across single targets, validating its utility for genome editing.

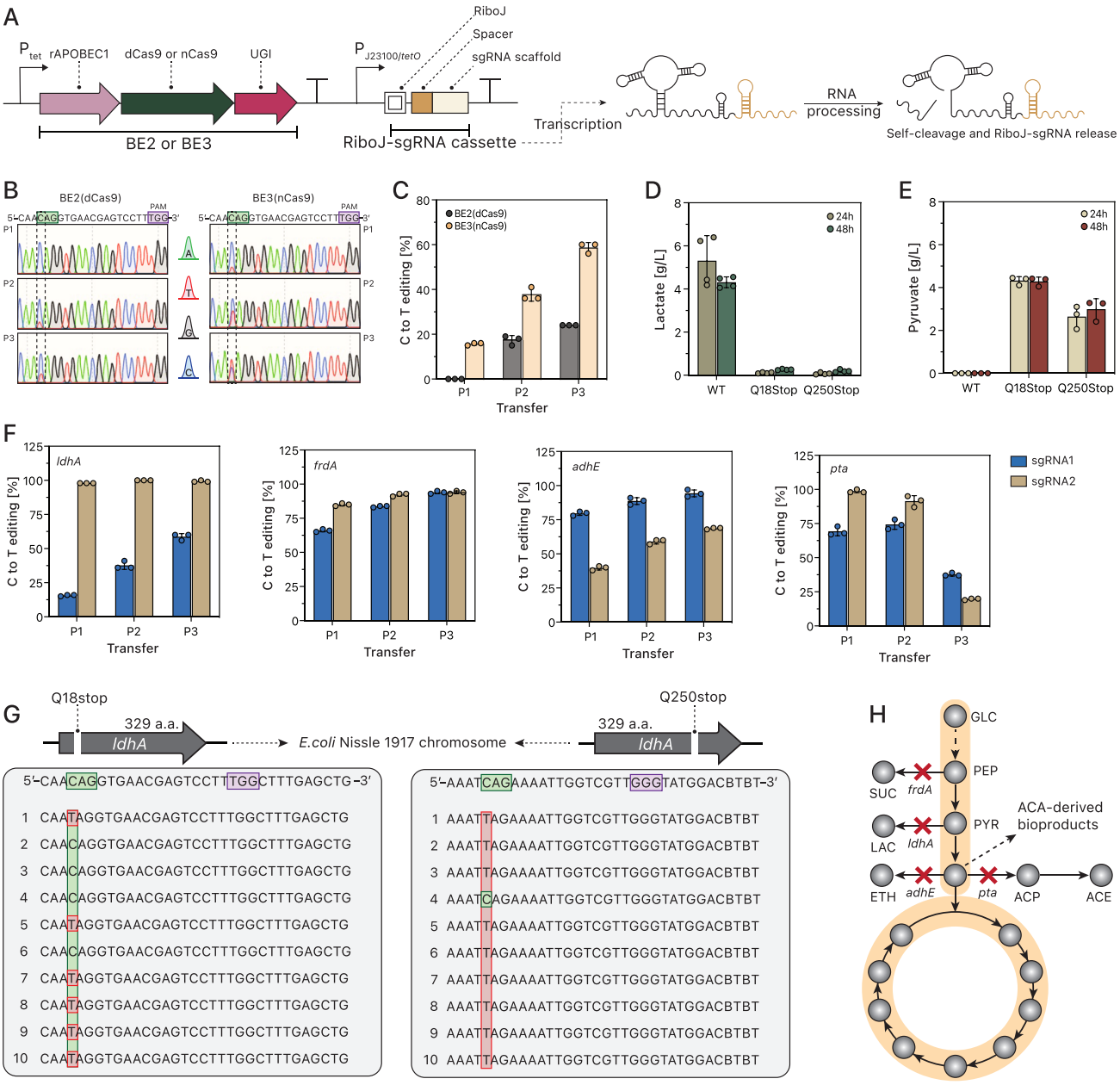

Fig. 1. Establishment of a RiboJ-aided base editing system. (A) The basic structures of the BE2 and BE3 systems as well as the RiboJ-sgRNA cassette are illustrated. Positioned downstream of the J23100/*tetO* promoter and upstream of a spacer sequence, the RiboJ component forms a part of the functional sgRNA in the RiboJ-sgRNA cassette. This cassette, which targets endogenous *ldhA* gene, is expressed through the J23100/*tetO* promoter in conjunction with BE2 or BE3 proteins. Following transcription, the primary RNA transcript undergoes self-cleavage by a RiboJ insulator, thereby generating functional sgRNA for base-editing alongside BE2 or BE3 proteins. (B) Representative Sanger sequencing chromatograms of the PCR amplicons within the *ldhA* gene are displayed, post-base-editing at each bacterial passage. The top DNA sequence represents the sgLdhA1 target sequence and its corresponding PAM recognition sequence (signified by the purple box). The black dotted rectangles highlight the target nucleotide and overlapping C/T peaks. The target CAG codon within the editing window is presented in a green box. (C) The C-to-T editing efficiencies for *ldhA* target were evaluated for BE2 and BE3 at each bacterial passage, using the EditR program. The mean and standard deviation (SD) of the data, collected from biological triplicates, are displayed. (D) The concentration of lactate in wild-type and *ldhA*-edited *Escherichia coli* Nissle 1917 (EcN) strains (Q18Stop and Q250Stop) was determined. The extracellular lactate concentration was gauged through high-performance liquid chromatography (HPLC) analysis after 24 and 48 h of cultivation in TB medium containing 10 g/L glucose, under micro-aerobic conditions. The mean and SD of the data, collected from biological triplicates, are presented. (E) The concentrations of pyruvate in wild-type and *ldhA*-edited EcN strains (Q18Stop and Q250Stop) were measured in the same way. (F) The simplex C-to-T editing efficiency was analysed for the introduction of a premature stop codon at the *ldhA*, *adhE*, *frdA*, and *pta* genes. The editing outcomes were scrutinized when the RAMBE system with BE3 was expressed at each bacterial passage. Quantification of C-to-T editing efficiency of endogenous genes for the two sets of sgRNAs was performed with the EditR program. The mean and SD of the data, collected from biological triplicates, are exhibited. (G) Sanger sequencing of PCR amplicons from 10 colonies and their alignment to the reference sequences for target sequences of sgLdhA1 and sgLdhA2 were performed. Base editing took place at *ldhA* gene using BE3-sgLdhA1 (left) or BE3-sgLdhA2 (right) to introduce premature stop codons (Q18Stop or Q250Stop), respectively, and the editing outcomes were verified using Sanger sequencing. The CAG codon within the editing window is highlighted in a green box, and the substituted bases are indicated with the red box. (H) The target genes for the RiboJ-aided base editing system are outlined, including four genes (*ldhA*, *adhE*, *frdA*, and *pta*) that contribute to the formation of byproducts from glucose in EcN. These genes encode a D-lactate dehydrogenase, an aldehyde-alcohol dehydrogenase, a fumarate reductase, and a phosphate acetyltransferase, respectively. The mean and SD of the data, again collected from biological triplicates, are shown. Detailed raw data and *p*-values are available in the Source Data File. (For interpretation of the references to colour in this figure legend, the reader is referred to the web version of this article.)

2.2. RAMBE-driven multiplex genome editing for improved butyrate production in EcN

Building on the success of single-target editing, we investigated whether RiboJ-mediated sgRNA processing could enable efficient multiplex editing of multiple genes from a single transcript. To achieve this, we developed the RAMBE system, which combines the BE3 protein, $P_{J23100/tetO}$ promoter, and a RiboJ-sgRNA array (Fig. 2A). This system was validated by targeting multiple genes associated with metabolic pathways in EcN.

The most efficient sgRNAs for *ldhA* and *adhE*, identified through single-target experiments (Fig. 1F), were incorporated into a single RiboJ-sgRNA array. Double-target editing achieved high C-to-T editing efficiencies of up to 99.5 % for *ldhA* and 98 % for *adhE*. Similarly, for *frdA* and *pta*, the RiboJ-sgRNA array achieved efficiencies of 84 % and 89 %, respectively (Fig. 2A). These results demonstrate the system's ability to process two sgRNAs from a single transcript, enabling simultaneous editing of two loci. To expand the system's capacity, we incorporated three sgRNAs targeting *ldhA*, *adhE*, and *frdA* into a single RiboJ-sgRNA array. The system achieved multiplex C-to-T editing efficiencies of 99.3 %, 97.3 %, and 97.3 %, respectively, across the three loci (Fig. 2B). The RAMBE system was further tested for quadruple-target genome editing by integrating sgRNAs targeting *ldhA*, *adhE*, *frdA*, and *pta*. Multiplex C-to-T conversion efficiencies reached 99.7 % for *ldhA*, 94 % for *adhE*, 92.7 % for *frdA*, and 67.7 % for *pta* (Fig. 2C). While the editing efficiency for *pta* decreased slightly, the overall performance of the system remained comparable to single-target experiments. These results demonstrate that RiboJ-mediated sgRNA arrays can support scalable genome editing with minimal loss in efficiency, enabling simultaneous editing of three genomic targets.

Following the base-editing process, edited EcN cells were plated onto LB plates to isolate single colonies with the desired genomic modifications and calculate multiplex BE efficiency. Interestingly, both large and small colonies were observed. Sanger sequencing revealed that the small colonies contained the desired stop codon mutation in the *pta* gene, while the large colonies exhibited a Q83K mutation caused by a rare C-to-A conversion (Fig. S4). These findings indicate that *pta* knockout suppresses cell growth, as the *pta* gene is critical for metabolic pathways involved in energy production and cell proliferation [51]. The disruption of *pta* likely interfered with the growth of correctly edited cells, resulting in an increased prevalence of cells with the Q83K mutation. The observed decline in editing efficiencies of *pta* over successive culture transfers can also be attributed to the negative effects of *pta* knockout on cellular growth (Fig. 1F). However, the *pta*-deficient EcN strain was easily isolated based on this distinct phenotypic feature. To assess editing outcomes at the target regions of the other three genes (*ldhA*, *adhE*, and *frdA*), we selected ten small colonies for further analysis. Sanger sequencing revealed that 80 % of the colonies exhibited a quadruple knockout frequency, while the remaining 20 % showed a triple knockout frequency (Fig. S5).

To evaluate the phenotypic impact of quadruple-target editing, EcN cells with early stop codons in *ldhA* (Q250X), *adhE* (W169X), *frdA* (Q96X), and *pta* (Q83X) (hereafter EcNΔLAFP) were isolated and analysed. The butyrate biosynthesis plasmid was introduced into EcNΔLAFP and wild-type EcN (EcNWT). The edited strain displayed significantly reduced byproduct formation (lactate, acetate, ethanol, and succinate) compared to the wild type. This shift in carbon distribution was further supported by biomass-normalized metabolite analysis, which showed increased butyrate production and reduced levels of byproducts in EcNΔLAFP compared to EcNWT (Fig. S6). Butyrate production reached 1.04 ± 0.12 g/L in EcNΔLAFP, representing a 7-fold increase compared to the 0.15 ± 0.02 g/L produced by EcNWT (Fig. 2E). These results demonstrate the potential of the RAMBE system for metabolic engineering applications.

To confirm the system's robustness across strains, the RAMBE plasmid targeting four genes (*ldhA*, *adhE*, *frdA*, *pta*) was transformed into *E. coli* MG1655. We analyzed five colonies, which revealed that 4 out of 5 exhibited quadruple knockouts, while one colony showed a triple knockout (Fig. S2). These findings highlight the versatility of the RAMBE system for genome editing in diverse *E. coli* strains. All multiplex base editing experiments were performed in a single step without intermediate clone selection. Editing efficiencies were measured directly from bulk populations, and individual colonies were isolated post-editing solely for validation purposes. Multiplex base editing efficiencies were determined from bulk populations without pre-screening of individual colonies. Single colonies were isolated after editing solely to validate the editing outcomes and phenotypes. The RiboJ-processed sgRNA arrays enable the simultaneous maturation of multiple sgRNAs from a single transcript, providing an efficient platform for parallel genetic modifications.

Butyrate is an important short-chain fatty acid with diverse applications, making it a high-value target for microbial production. It serves as a precursor for biofuels, bioplastics, and other renewable chemicals, offering sustainable alternatives to petrochemical-derived products [52]. Butyrate also plays a crucial role in human health as a therapeutic molecule, particularly for gut-related disorders such as inflammatory bowel disease and colorectal cancer [53]. Additionally, butyrate acts as an epigenetic regulator by inhibiting histone deacetylases, which has therapeutic implications in neurodegenerative diseases and cancer treatment [54]. In this study, the successful application of the RAMBE system to both EcN and *E. coli* MG1655 underscores its versatility in engineering microbial cell factories for butyrate production. By enabling precise and efficient multiplex genome editing, the RAMBE system optimizes key metabolic pathways, significantly enhancing butyrate yield while reducing unwanted byproducts. This advancement highlights the system's potential for developing scalable microbial platforms tailored to produce butyrate and its derivatives for industrial and therapeutic purposes.

2.3. RAMBE-driven multiplex genome editing for improved acetate utilization in EcN

To investigate the scalability of the RAMBE system, we sought to determine its ability to introduce simultaneous C-to-T base conversions in six endogenous genes. Our earlier work demonstrated that knocking out the *cspC* and *patZ* genes in DSM01 (*E. coli*Δ*frdA*Δ*pta*Δ*ldhA*Δ*adhE*) enhanced acetate utilization and increased intracellular ATP levels, improving bioproduct production from acetate [55]. Based on these findings, *cspC* and *patZ* in EcN were selected as additional targets for introducing premature stop codons using C-to-T base editing (Fig. 3B). Two sgRNAs (sgCspC1, sgCspC2) were designed to introduce the Q48X mutation in *cspC*. Over three culture transfers, editing efficiencies reached 58.3 % and 28 %, respectively. Similarly, sgPatZ1 and sgPatZ2 targeted *patZ*, achieving editing efficiencies of 100 % and 22.7 %, respectively (Fig. 3A). These results highlight the capability of the RAMBE system to introduce precise edits at multiple loci. To address the PAM limitations of standard BE3, we utilized an SpCas9n variant (VRVRFRR), referred to as BE3-NG, which recognizes NG PAMs [56]. Using this system, we targeted previously inaccessible sites in *cspC* (Q7X, Q48X, Q58X) and *patZ* (W501X). sgCspC3, sgCspC4, and sgCspC5 achieved editing efficiencies of 89 %, 27.7 %, and 29.3 %, respectively, while sgPatZ3 and sgPatZ4 (22-nt and 20-nt spacers) both reached 84.3 % (Fig. 3A). These results demonstrate the versatility of BE3-NG in expanding editable loci and enabling efficient base editing.

To evaluate the RAMBE system's ability to edit multiple genes simultaneously, six sgRNAs (*ldhA*, *adhE*, *frdA*, *pta*, *cspC*, *patZ*) were integrated into a single RiboJ-sgRNA array. The RiboJ-sgRNA array successfully processed all six sgRNAs from a single transcript, achieving high multiplex editing efficiencies of 99 %, 96 %, 93.7 %, 83.7 %, 33.3 %, and 99 %, respectively, across the six loci (Fig. 3C). Except for *cspC*, these efficiencies were comparable to those observed in single target editing experiments. Furthermore, editing efficiencies measured by

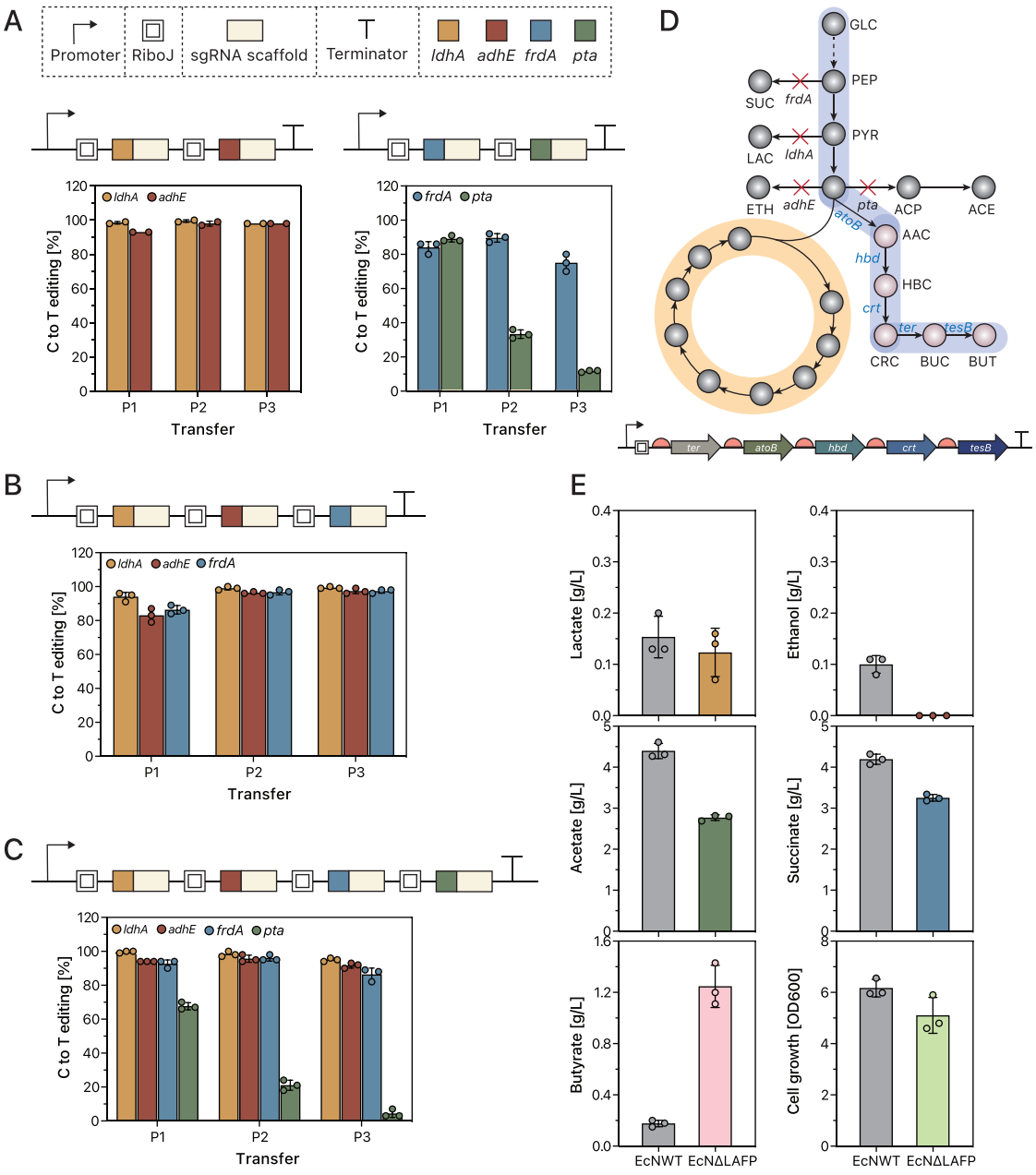

Fig. 2. Multiplex genome editing using the RAMBE system. (A) Double-target genes. The composition of RiboJ-sgRNA arrays, including alternating RiboJ insulators, a pair of gene-specific spacers, conserved sgRNA scaffolds, and the J23100/*tetO* promoter, is displayed for double-target genes. The multiplex C-to-T editing efficiencies mediated by the RAMBE system for these dual-target genes are presented as bar graphs, featuring mean and standard deviation (SD) values derived from three biological replicates for each gene pair. By adding 250 nM aTc at each bacterial passage, BE3 and RiboJ-sgRNA array were co-expressed. The EditR program quantified the multiplexed C-to-T editing efficiencies for the two distinct gene pairs. The illustrations continue with (B) triple-target genes and (C) quadruple-target genes. The multiplex C-to-T editing efficiencies for these multiple-target genes, mediated by the RAMBE system, are evaluated in the same way. (D) The diagram provides an overview of the heterologous butyrate synthesis pathway, highlighting in blue the heterologous genes for butyrate production. These include *atoB* (an acetoacetyl-CoA thiolase-encoding gene sourced from *E. coli*), *hbd* and *crt* (encoding 3-hydroxybutyryl-CoA dehydrogenase and 3-hydroxybutyryl-CoA dehydratase, respectively; both derived from *Clostridium acetobutylicum*), *ter* (a *trans*-enoyl-coenzyme A reductase-encoding gene from *Treponema denticola*), and TesB (an acyl-CoA thioesterase II encoding gene sourced from *E. coli*). A plasmid depicting the butyrate synthesis is showcased, containing the *ter*, *atoB*, *hbd*, *crt*, and *tesB* genes. The P_{trc} promoter regulates the expression of all heterologous genes. (E) Comparisons between the wild-type EcN (EcNWT) and the quadruple base-edited EcNΔLAFP strains were made, focusing on cell growth and concentrations of butyrate and byproducts such as lactate, acetate, ethanol, and succinate. Shaking-flask production was carried out in terrific broth (TB) medium with 5 g/L glucose under micro-aerobic conditions. Cell growth and concentrations of extracellular butyrate and byproducts were monitored during the 48 h of micro-aerobic cultivation. The data denote the mean and SD of butyrate concentrations from biological triplicates for both the EcNWT and EcNΔLAFP strains. Detailed raw data and *p*-values are available in the Source Data File. (For interpretation of the references to colour in this figure legend, the reader is referred to the web version of this article.)

Sanger sequencing and EditR were consistent with the next-generation sequencing (NGS) results (Fig. S3), indicating reliable and reproducible base editing across multiplex targets. Notably, incorporating RiboJ into the sgRNA array significantly improved editing efficiency across all targets compared to arrays without RiboJ (Fig. S3). Interestingly, base editing was still detectable even without RiboJ, suggesting that other

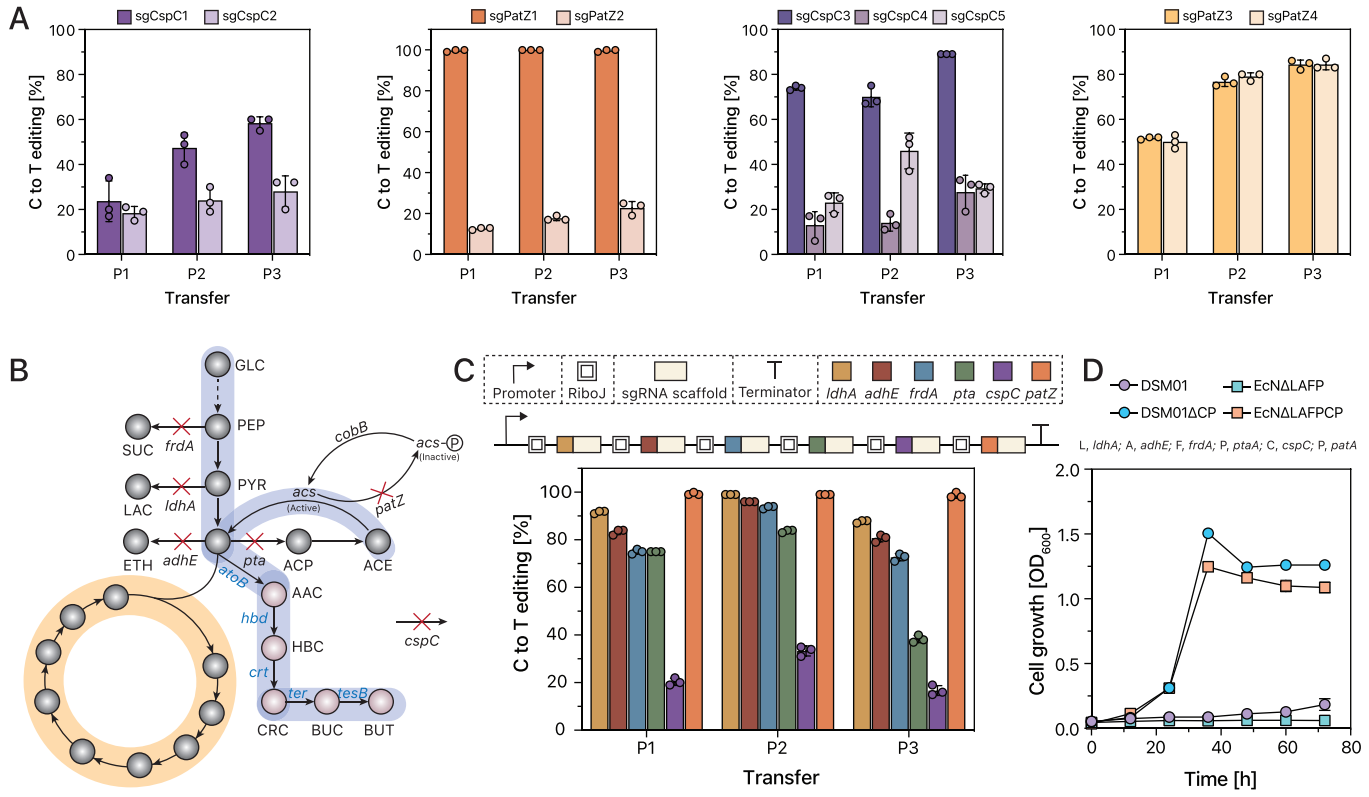

Fig. 3. Multiplex genome editing capability of the RAMBE system, enabling simultaneous knockout of six target genes. (A) The simplex C-to-T editing efficiency is evaluated for the introduction of a premature stop codon at *cspC* and *patZ* genes. Editing outcomes for *cspC* and *patZ* targets were analysed when the RiboJ-facilitated genome editing system with BE3 was employed. The RAMBE system's versatility was further expanded by relaxing the necessity for PAMs. The editing outcomes for *cspC* and *patZ* targets were re-evaluated using the BE3-NG in the RiboJ-aided genome editing system, again for the introduction of a premature stop codon. Quantitative assessment of the C-to-T editing efficiency of endogenous genes for a set of sgRNAs was accomplished with the EditR program at each bacterial passage. The mean and SD of the data, gathered from biological triplicates, are displayed. (B) The diagram offers a synopsis of the heterologous butyrate synthesis pathway (*atoB*, *hbd*, *crt*, *ter*, and *tesB*) and six target genes (*ldhA*, *frdA*, *adhE*, *pta*, *cspC*, and *patZ*), previously recognised for enabling the *E. coli* strain to utilise acetate as a sole carbon .

Source. (C) A visual representation of the RiboJ-sgRNA array, consisting of alternating RiboJ insulators, six gene-specific spacers, conserved sgRNA scaffolds, and the J23100/*tetO* promoter, is provided. The multiplex C-to-T editing efficiencies, mediated by the RAMBE system, for the six target genes (*ldhA/adhE/frdA/pta/cspC/patZ*) are depicted as bar graphs with mean and SD values, based on three biological replicates for each gene pair. The BE3 and RiboJ-sgRNA array were co-expressed by administering 250 nM aTc at each passage. The EditR program was used to determine the multiplexed C-to-T editing efficiencies for the six distinct gene pairs. (D) Growth profiles of various *E. coli* strains in M9 acetate minimal medium are presented. The cell growth (OD_{600}) of DSM01, DSM01Δ*cspC*Δ*patZ*, EcNΔ*ldhA*-Δ*adhE*Δ*frdA*Δ*pta*, and EcNΔLAFPCP strains was observed in M9 minimal medium, with acetate serving as the sole carbon source, using a UV–VIS spectrophotometer. The mean and SD of the data, obtained from biological triplicates, are displayed. Detailed raw data and *p*-values are available in the Source Data File

mechanisms might compensate for the lack of ribozyme-mediated processing. This observation suggests that transcription and processing can still proceed to some extent without RiboJ, possibly due to internal transcription initiation within the array. A previous study [57] reported that gRNA arrays could self-transcribe without a promoter, likely because promoter-derived target sequences facilitated internal transcription initiation. This could explain why base editing was still detectable in the absence of RiboJ elements in our array.

To assess the functional impact of simultaneous editing, we constructed an EcN strain with stop codons in *ldhA*, *adhE*, *frdA*, *pta*, *cspC*, and *patZ* (EcNΔLAFPCP). Growth assays in M9 minimal medium with acetate as the sole carbon source revealed that EcNΔLAFPCP and DSM01Δ*cspC*Δ*patZ* could grow under these conditions, whereas DSM01 and EcNΔLAFP could not, consistent with previous findings [55]. This demonstrates that *cspC* and *patZ* knockouts restore acetate utilization (Fig. 3D). By reducing byproduct formation and enhancing metabolic flux toward acetyl-CoA, the RAMBE-edited strains exhibited improved butyrate production and acetate utilization.

Acetate is a key intermediate in microbial metabolism and an important substrate in metabolic engineering, particularly to produce value-added chemicals. It serves as a precursor for a variety of industrial products, including biofuels, bioplastics, and organic acids, offering sustainable alternatives to petroleum-based processes [58–60]. In addition to its industrial applications, acetate is a critical component of the gut microbiome, where it can be metabolized into beneficial molecules like butyrate [61]. This acetate-to-butyrate conversion is especially significant for maintaining gut health and treating disorders such as inflammatory bowel disease and metabolic syndrome [62]. In this study, the successful application of the RAMBE system to *E. coli* strains, including EcN and MG1655, highlights its potential for optimizing acetate utilization pathways. By engineering these pathways, the system not only enhances acetate utilization but also redirects metabolic flux toward high-value products like butyrate, demonstrating its versatility and scalability for advanced genome engineering applications including metabolic engineering and development of therapeutic microbes.

2.4. Establishment of a Non-Repetitive RAMBE (NR-RAMBE) system

Constructing CRISPR arrays presents significant challenges due to their repetitive nature, which consists of alternating spacers and repeats. These sequences complicate assembly, often requiring labor-intensive cloning methods such as Golden Gate assembly [15,21,63]. As the number of targets increases, the process becomes inefficient, error-prone, and less adaptable for large-scale applications [15,21].

To address these limitations, we developed a streamlined approach for sgRNA array synthesis through gene synthesis, eliminating the need for complex assembly methods. This led to the design of the NR-RAMBE system, which incorporates diverse ribozymes and engineered non-repetitive sgRNA handles, effectively reducing sequence repetition while maintaining functional efficiency. Our approach was inspired by previous computational work on the CRISPRi system [37], which focused on non-repetitive engineering of sgRNA sequences, particularly in the repeat: anti-repeat duplex (RAR), stem loop (SL) 1 (SL1), and SL2, but not SL3. However, this CRISPRi assay is monocistronic, requiring separate non-repetitive promoters and transcriptional terminators for each sgRNA, which limits its applicability due to the need for multiple distinct promoters and terminators. In contrast, our RiboJ-based sgRNA array is polycistronic, requiring only a single promoter and terminator along with engineered non-repetitive elements. This design potentially broadens the applicability of the NR-RAMBE system to a wide range of prokaryotic organisms beyond *E. coli*.

To evaluate ribozyme performance in the NR-RAMBE system, we tested 15 different ribozymes using a GFP reporter assay, where base editing converted the silent start codon (ACG) of GFP to ATG (Fig. 4A). Among the tested ribozymes, 12 significantly increased GFP-positive cell populations by over 70 % upon aTc induction, confirming their efficiency in sgRNA processing (Fig. 4B). Additionally, we truncated unnecessary hairpin loops from ribozymes, optimizing their structure for improved performance. Among various RiboJ variants tested, RiboJ (T1), which included an extra 4-bp sequence (total length of 57 bp), exhibited the highest GFP-positive cell population at 89.5 % (Fig. 4C, 4D). Similarly, eight truncated ribozymes significantly increased GFP-positive cell populations to over 80 %, demonstrating their suitability for further applications (Fig. 4F).

To minimize repetitive sequences in sgRNA handles while ensuring functional efficiency, we focused on modifying the SL3 region. While SL1 is essential for forming the Cas9-sgRNA complex, SL2 and SL3 contribute to its stability, with SL3 playing a critical role in Cas9 cleavage efficiency [64]. We designed various SL3 variants capable of forming a functional stem structure and compared their performance using the GFP reporter system (Fig. 4E). All SL3 variants showed comparable GFP-positive cell populations, confirming their functional activity (Fig. 4G). To further enhance non-repetitive sgRNA handle design, we combined SL3 variants with previously optimized SL1 and SL2 regions [37], generating 72 novel non-repetitive sgRNA handles. Among these, 38 significantly increased GFP-positive cell populations to over 80 % following aTc induction (Fig. 4H). This demonstrates the effectiveness of combining engineered sgRNA handles with NR-RAMBE for reducing sequence repetition while maintaining high functionality.

By integrating diverse ribozymes and optimized non-repetitive sgRNA handles, the NR-RAMBE system addresses key challenges in CRISPR multiplexing. The use of polycistronic sgRNA arrays eliminates the need for separate promoters and terminators for each sgRNA, simplifying design and enabling broader applicability across different organisms. Additionally, the NR-RAMBE system enhances sgRNA stability and processing efficiency, ensuring reliable Cas9-sgRNA complex formation and activity. These findings highlight the NR-RAMBE system as a robust platform for high-efficiency genome editing. By minimizing repetitive sequences and optimizing sgRNA processing, the system improves the scalability and stability of sgRNA arrays, providing a powerful tool for synthetic biology and metabolic engineering.

2.5. Application of the NR-RAMBE system for multiplex genome editing

To evaluate the multiplex genome editing capabilities of the NR-RAMBE system, six sgRNAs (*ldhA*, *adhE*, *frdA*, *pta*, *cspC*, and *patZ*) were incorporated into a single engineered ribozyme-sgRNA array. This array was assembled into a BE plasmid in a single step using Gibson Assembly, eliminating the need for labor-intensive multi-step cloning methods (Fig. 5A). The streamlined workflow highlights the efficiency of NR-RAMBE for sgRNA array synthesis and assembly, simplifying the process for genome engineering applications. The engineered ribozyme-sgRNA array enabled the simultaneous processing of all six sgRNAs from a single transcript. This facilitated precise C-to-T base editing at the target regions of all six genes, achieving editing efficiencies of 80.7 %, 100 %, 82.3 %, 54.7 %, 17 %, and 78.3 % for *ldhA*, *adhE*, *frdA*, *pta*, *cspC*, and *patZ*, respectively (Fig. 5B). Notably, these multiplex editing efficiencies were comparable to those achieved with the original RAMBE system, demonstrating that the non-repetitive ribozyme-sgRNA design does not compromise editing performance. In addition to its multiplexing efficiency, the NR-RAMBE system was successfully applied to EcN, a probiotic strain widely studied for its diagnostic and therapeutic potential [43,44]. Historically, EcN's resistance to genetic modification posed challenges for its use in synthetic biology [45]. However, the NR-RAMBE system effectively overcame these barriers, enabling precise and efficient genome editing in EcN. This demonstrates the platform's robustness and adaptability for challenging bacterial systems. These results underscore the NR-RAMBE system as a powerful and versatile genome editing platform. By facilitating multiplex editing with a non-repetitive ribozyme-sgRNA design, the system simplifies workflows while maintaining high editing efficiencies. Its successful application to EcN further broadens its potential for synthetic biology and genetic engineering, providing a robust tool for both fundamental and applied research.

2.6. Comparative analysis of repetitive and non-repetitive sgRNA arrays

To comprehensively evaluate the advantages of the NR-RAMBE system over its predecessor, we conducted a comparative analysis of the repetitive sgRNA array (R6) from the RAMBE system and the non-repetitive sgRNA array (N6) from the NR-RAMBE system (Fig. 5C, Supplementary Table 1). The DNA sequences of both arrays are detailed in Supplementary Table 6. This analysis was conducted in collaboration with Macrogen (Korea) and IDT (USA), leveraging their expertise in oligonucleotide synthesis and sequence complexity assessment. The R6 array (1,036 bp, 43 % GC) contained extensive repetitive sequences, including six 171-bp tandem repeats (91 % identity) and interspersed repeats totaling 918 bp, resulting in a total repeat content of 1,944 bp (Fig. 5C and Supplementary Table 1). This high redundancy led to repeated synthesis failures reported by Macrogen due to sequence instability, a known challenge in synthesizing tandem repeat-rich DNA. Complexity analysis by IDT further confirmed the synthetic difficulty, assigning the R6 array a complexity score of 300.9. In contrast, the N6 array (992 bp, 46 % GC) eliminated tandem repeats and reduced interspersed repeats to 194 bp (Fig. 5C and Supplementary Table 1), enabling efficient synthesis and improved sequence stability.

This streamlined structure resulted in a lower synthesis complexity score of 13, as evaluated by IDT, compared to 300.9 for the R6 array. The complexity score is a vendor-specific internal metric that reflects synthesis difficulty based on sequence features such as repeats and GC content. Although this reflects a 23-fold difference in the assigned complexity scores, it should be interpreted as a vendor-specific estimation rather than a universal quantitative measure of synthesis complexity. Nevertheless, this stark difference clearly demonstrates the advantage of the non-repetitive design in facilitating array synthesis and reducing the complexity burden for downstream applications. Notably, a recent study also utilized IDT's complexity score to assess synthesis feasibility, where sequences with high complexity scores (ranging from 30 to 139) failed synthesis screening due to repetitive elements [65]. Macrogen successfully synthesized the N6 array with a turnaround time of 10–15 working days, at significantly reduced costs compared to the R6 array. These findings underscore the practical advantages of the NR-RAMBE system in facilitating the efficient and cost-effective synthesis of complex sgRNA arrays.

The NR-RAMBE system's non-repetitive design, incorporating optimized sgRNA handles, simplifies in vitro synthesis processes while

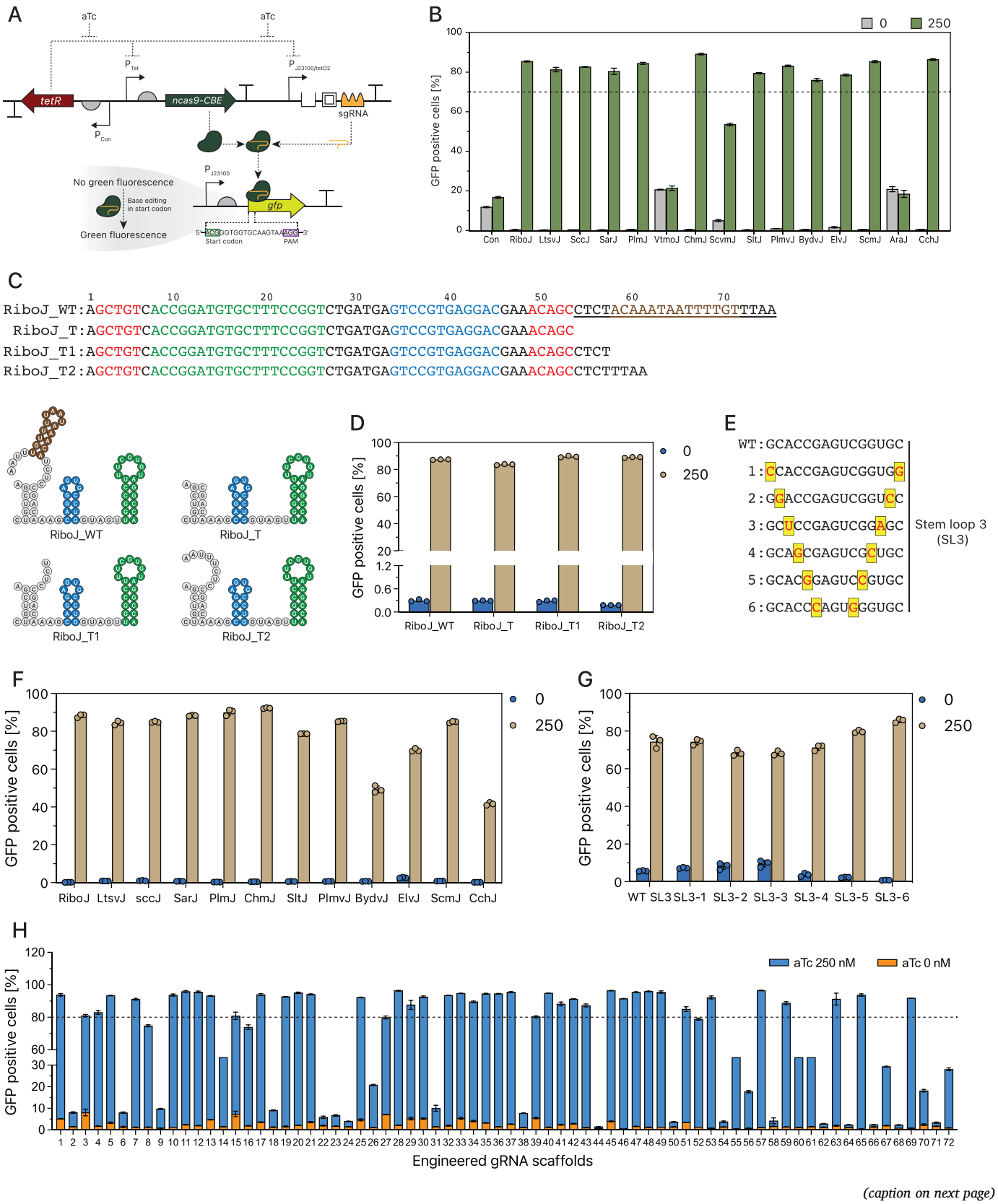

(caption on next page)

Fig. 4. Development of the NR-RAMBE system. (A) Genetic circuit to sense cytosine base-editing activity. Both BE3 and RiboJ-sgRNA are expressed under the regulation of the promoters that respond to aTc. The reporter plasmid includes a silent *gfp* gene cassette driven by a constitutive J23100 promoter. BE3 and sgRNA form a complex and target the mutated start codon (ACG) of the silent *gfp* gene in the reporter plasmid, leading to a C-to-T base conversion (ACG → ATG). The percentage of GFP-positive cells was analysed using a flow cytometer to monitor the base-editing activity. The target nucleotide (ACG) and PAM sequence (AGG) are indicated in green and purple, respectively. (B) Screening of diverse ribozymes for base-editing. The ratio of GFP-positive cells to untransformed cells was measured using flow cytometry, both with and without 250 nM aTc. Con indicates construct without ribozyme. The same settings were used for all constructs. The mean and standard deviation (SD) of the data from biological triplicates is presented. (C) A panel of RiboJ variants is presented, along with their remaining hairpin loop sequences. The green and blue residues represent stems I and II, respectively, whereas the conserved catalytic core is represented by red residues. The stem-loop of the additional hairpin is indicated by orange residues. To reduce the length of the remaining sequence, the underlined portions were truncated. (D) The impact of RiboJ variants on base-editing activity was assessed using flow cytometry. The population of GFP-positive cells relative to untransformed control cells was monitored using flow cytometry with or without 250 nM aTc. Identical settings were used for all constructs. The data represent the mean and SD from biological triplicates. (E) Stem-loop 3 variants with mutated sequences are presented. The original (WT) stem-loop 3 of sgRNA scaffold was altered to the indicated sequence pair to decrease consecutive repetitive sequences. (F) Flow cytometry was used to screen for the impact of a panel of truncated ribozymes on base-editing activity. The ratio of GFP-positive cells to untransformed control cells was measured using flow cytometry, both with and without 250 nM aTc. The same settings were used for all constructs. The mean and SD of the data from biological triplicates is presented. (G) Flow cytometry was used to evaluate the effect of stem-loop 3 engineering on base-editing activity. The ratio of GFP-positive cells to untransformed control cells was measured by flow cytometry with or without 250 nM aTc. Identical settings were used for all constructs. The mean and SD of the data from biological triplicates are shown. (H) Flow cytometry was used to evaluate the effect of sgRNA scaffold engineering on base-editing activity. The ratio of GFP-positive cells to untransformed control cells was measured by flow cytometry with or without 250 nM aTc. Identical settings were used for all constructs. The mean and SD of the data from biological triplicates are shown. Detailed raw data and *p*-values are available in the Source Data File. (For interpretation of the references to colour in this figure legend, the reader is referred to the web version of this article.)

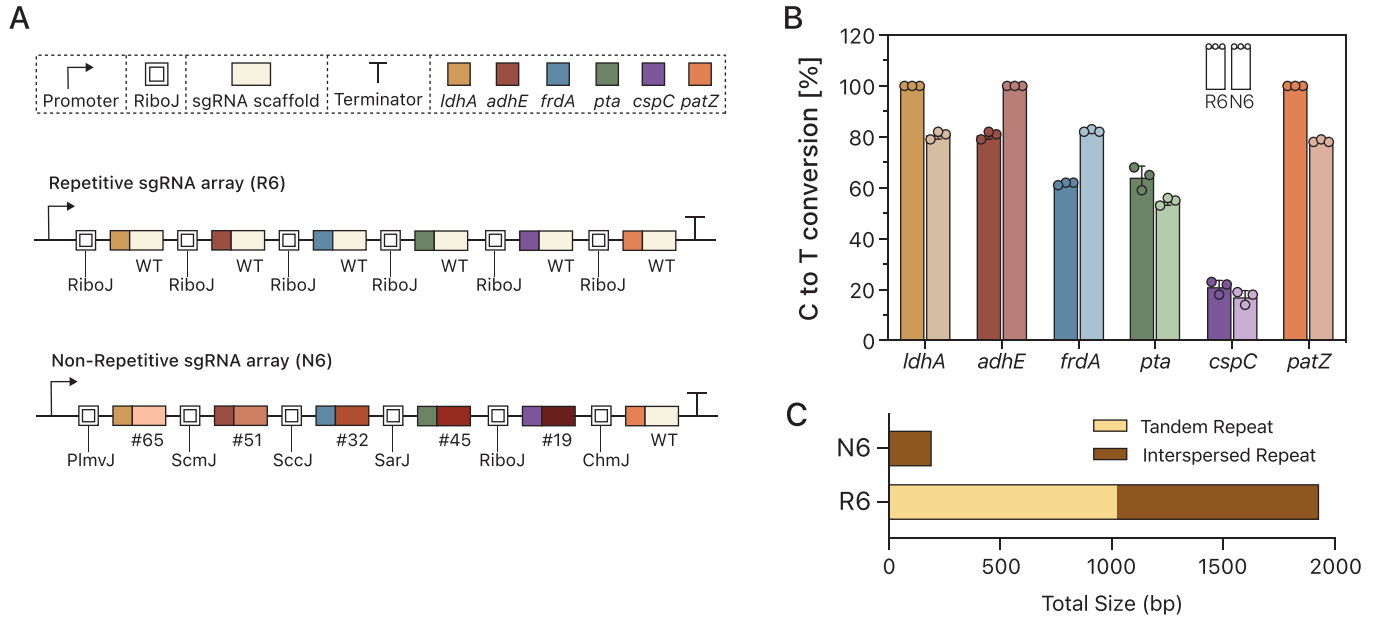

Fig. 5. Comparison of RAMBE and NR-RAMBE. Development and characterization of the NR-RAMBE system. (A) Graphical representation of the repetitive sgRNA array (called R6) and non-repetitive sgRNA array (called N6) is presented. R6 was generated by using six repetitive RiboJ-sgRNA arrays with the J23100/*tetO* promoter; N6 was generated by using six combinations of different ribozymes and engineered sgRNA scaffolds with the J23100/*tetO* promoter. (B) Quantification of multiplexed C-to-T editing efficiencies for the six target genes (*ldhA/adhE/frdA/pta/cspC/patZ*) using the R6 or N6 are presented as bar graphs with mean and standard deviation (SD) values based on three biological replicates for each gene pair. The BE3-R6 or −N6 were expressed by adding 250 nM aTc. The EditR program was used to quantify the multiplexed C-to-T editing efficiencies for the six distinct gene pairs. (C) Quantification of tandem and interspersed repeats in the R6 and N6 arrays. The bar graph illustrates the total size of tandem and interspersed repeats in the R6 and N6 arrays. The R6 array contains six 171-bp tandem repeats (91 % identity) and 918 bp of interspersed repeats, leading to high sequence redundancy. In contrast, the N6 array eliminates tandem repeats and reduces interspersed repeats to 194 bp. Repeat profiling is based on Supplementary Table 1. Detailed raw data and *p*-values are available in the Source Data File.

significantly reducing both time and financial costs. These features are particularly advantageous for large-scale genomic projects and multiplex CRISPR-Cas applications, where the ability to efficiently construct complex sgRNA arrays is critical. Despite these advancements, minor residual repeats of up to 23 bp remain in the NR-RAMBE design, which could still pose a risk of homologous recombination, particularly in large-scale arrays or highly recombinogenic hosts. To address this, future work will focus on further engineering of sgRNA handles and ribozyme sequences to eliminate these residual repeats and minimize recombination risks. Additionally, ribozyme cleavage efficiency may vary depending on host-specific RNA processing environments, potentially affecting sgRNA maturation. Alternative ribozyme designs or synthetic RNA processing systems could be explored to ensure robust performance across diverse microbial hosts. These improvements will further enhance the scalability, stability, and broad applicability of the NR-RAMBE system for complex genome engineering tasks. Such improvements are anticipated to further enhance the precision, efficiency, and scalability of the system. By overcoming the inherent limitations associated with repetitive DNA sequences, the NR-RAMBE system represents a transformative leap in multiplex genome editing technology. The system's non-repetitive architecture not only ensures high fidelity in sgRNA processing but also provides a robust and scalable platform for precise genetic modifications. With its demonstrated efficiency and scalability, the NR-RAMBE system unlocks new possibilities for intricate genome manipulations across diverse applications in synthetic biology, metabolic engineering, and therapeutic development. This innovation

stands as a critical advancement in CRISPR-Cas systems, addressing key barriers to multiplex genome editing and paving the way for more efficient and versatile genomic engineering platforms.

Furthermore, previous studies have reported Cas12a-based multiplex genome editing platforms that leverage the intrinsic RNase activity of Cas12a to efficiently process crRNA arrays. In human cells, simultaneous editing of up to four genes was demonstrated using a single crRNA array processed by Cas12a, with editing efficiencies ranging from 40 % to 70 % at each target site [22]. Multiplexed genome engineering has also been achieved by encoding CRISPR arrays on single transcripts, enabling editing of up to five loci in mammalian cells with efficiencies reaching 80 % [23]. In microbial systems, Cas12a-based methods facilitated combinatorial editing and transcriptional regulation, with correct array assembly rates ranging from 60 % to 100 % and editing efficiencies of up to 100 %, depending on the target and context [21]. While these Cas12a-based systems offer scalable multiplex editing, their utility is inherently limited by stringent PAM requirements and the challenges of repetitive crRNA array design. In contrast, our NR-RAMBE system provides broader flexibility by enabling multiplex base editing with engineered non-repetitive sgRNA arrays, independent of Cas12a's processing mechanism. This design expands its potential applicability to a wider range of organisms and genome editing contexts.

To further investigate sgRNA abundance and processing efficiency within the multiplex array, we plan to perform RNA-seq analysis in future studies. This will allow direct quantification of each sgRNA and provide deeper insights into the stoichiometry and potential bottlenecks of our multiplex base editing system. Additionally, we plan to perform whole-genome sequencing (WGS) to comprehensively assess potential off-target effects and further validate the specificity and safety of our multiplex base editing platform.

3. Conclusions

This study presents the RAMBE and NR-RAMBE systems as innovative platforms for multiplex genome editing, highlighting novel contributions through the systematic design and screening of RiboJ-based sgRNA processing and non-repetitive sgRNA handles. For the first time, a wide array of ribozymes and sgRNA scaffolds were combined and evaluated, enabling the development of diverse configurations that address key limitations of repetitive DNA sequences, including synthesis complexity and stability challenges. The NR-RAMBE system reduces synthesis complexity by 23-fold while maintaining comparable editing efficiencies to repetitive designs, demonstrating its potential for scalable applications. Although the system currently focuses on *E. coli*, its design principles can be extended to other cell types and organisms, paving the way for broader applications in synthetic biology and metabolic engineering. By facilitating precise and efficient multiplex editing, this study establishes the RAMBE and NR-RAMBE systems as robust tools for advancing genome editing technologies, enabling new opportunities for developing microbial cell factories, therapeutic microbes, and high-throughput genetic studies. Future efforts will focus on expanding the system's applicability to diverse organisms and further optimizing gRNA array design to enhance its versatility and precision.

4. Materials and methods

4.1. Bacterial strains and growth conditions

The bacterial strains used in this study are listed in Supplementary Table 2. *E. coli* strains were employed for plasmid cloning, propagation, base-editing experiments, and butyrate production, as detailed in the text. Bacteria were cultured in LB (containing 10 g/L tryptone, 5 g/L yeast extract, and 10 g/L sodium chloride) at 37 °C, with agitation at 200 rpm, unless noted otherwise. *E. coli* strains were additionally cultivated in TB medium, comprising 12 g/L tryptone, 24 g/L yeast extract, 9.4 g/L K_2HPO_4, and 2.2 g/L KH_2PO_4, under micro-aerobic conditions. This medium was supplemented with 5 g/L glucose to verify butyrate production and with 10 g/L glucose to verify lactate and pyruvate concentrations. If required, antibiotics (100 μg/mL ampicillin or 50 μg/mL kanamycin), anhydrotetracycline (aTc), and isopropyl-β-D-1-thiogalactopyranoside (IPTG) were incorporated into the medium. Following transformation, super-optimal broth with catabolite repression (SOC) medium was used for recovery. Restriction enzymes were sourced from New England BioLabs (NEB, Ipswich, MA, USA) and all analytical-grade reagents were procured from Sigma-Aldrich (St. Louis, MO, USA).

4.2. Plasmid construction

The complete list of plasmids used in this study is shown in Supplementary Table 2, and DNA oligonucleotides synthesised by Macrogen (Seoul, Korea) are provided in Supplementary Table 3. Unless otherwise specified, all the recombinant plasmids were constructed using the Gibson Assembly method. Supplementary Table 4 lists the sgRNA-binding sites used in this study. Standard protocols were followed for PCR amplification using KOD Plus Neo (Toyobo, Code No. KOD-401), or KOD One PCR Master Mix (Toyobo, Code No. KMM-201). Three plasmids were synthesised: pTet-BE2-sgLdhA1 with APOBEC1-dCas9-UGI and sgRNA cassettes, pTet-BE3-sgLdhA1 with APOBEC1-nCas9-UGI and sgRNA cassettes, and pRAMBE(NG) with APOBEC1-nCas9 variant (VRVRFRR)-UGI and sgRNA cassettes (Supplementary Table 5). The F1, F2, and F3 fragments were produced by PCR of the synthesized DNA, PCR of the pSECRi plasmid, and XbaI/PacI digestion of pSECRi, respectively. These fragments were assembled using Gibson Assembly to generate plasmids. The pTet-BE3-sgLdhA1 plasmid was digested with XhoI and PacI. The appropriate bands were extracted and purified using the LaboPass Gel and PCR Clean-up Kit (CosmoGenetech, Seoul, Korea) according to the manufacturer's instructions. This purified vector served as the backbone plasmid for constructing pRAMBE derivatives, unless stated otherwise. Single-target editing plasmids were constructed by PCR amplification from the pTet-BE3-sgLdhA1 plasmid with the primers pTet-sg(XhoI)-F and J23100(tetO)-RiboJ-R. The PCR fragment was treated with DpnI and purified using the LaboPass Gel and PCR Clean-up Kit (Cosmo Genetech). To easily replace the sgRNA spacer for each target gene, primers S(target gene)-F and pTet-sg(PacI)-R were used for PCR amplification from the pTet-BE3-sgLdhA1 plasmid. The resulting fragments were assembled into the pRAMBE backbone plasmid using the Gibson Assembly method. Double-target editing plasmids (pRAMBE-D1, −D2, and-D3) were constructed by PCR amplification of the pRAMBE-sgLdhA2,-sgFrdA2, and-sgCspC1 plasmids using the primers pTet-sg (XhoI)-F and D-R. D-F and pTet-sg(PacI)-R primer pairs were used for PCR amplification of the pRAMBE-sgAdhE2, −sgPta2, and –sgPatZ1 plasmids. The resulting fragments were assembled into the pRAMBE backbone plasmid using the Gibson Assembly method. To create the triple-target editing plasmid, the pRAMBE-D1 plasmid was digested with NotI-HF and PacI and the backbone plasmid was extracted via gel electrophoresis. PCR amplification from the pRAMBE-sgFrdA2 plasmid utilised the M(NotI)-F and pTet-sg(PacI)-R primers. The two resulting fragments were combined using the Gibson Assembly method to generate the pRAMBE-T plasmid. To construct the quadruple-target editing plasmid, the pRAMBE-T plasmid was digested with NotI-HF and PacI, followed by backbone plasmid gel extraction. PCR amplification of the pRAMBE-sgPta2 plasmid was performed using the M(NotI)-F and pTet-sg(PacI)-R primers. The two extracted fragments were assembled using the Gibson Assembly method to obtain the pRAMBE-Q plasmid. Finally, to construct the pRAMBE-M plasmid, the pRAMBE-Q plasmid was digested with NotI-HF and PacI and the backbone plasmid was extracted via gel electrophoresis. Primers M (NotI)-F and pTet-sg (PacI)-R were used for PCR amplification of the pRAMBE-D3 plasmid. The two fragments were combined using the Gibson Assembly method. To generate the pSETR-butyrate plasmid, genes involved in butyrate production (*ter*, *atoB*, *hbd*, *crt*, and *tesB*) were PCR-amplified

from pAB-AHCTA using their respective primer pairs. The PCR products were assembled into the pTrc99A vector using the Gibson Assembly method to generate the plasmids pTSN-ter-atoB, pTSN-hbd-crt, and pTSN-tesB. A fragment containing all five genes was amplified and incorporated into pTrc99A to form the pTSN-butyrate plasmid. To swap the origin of replication, the pTSN-butyrate plasmid was digested with XbaI and ApaI followed by backbone plasmid gel extraction. PCR amplification of the pSEVA131 plasmid used pBBR1(XbaI)-F/R primers, whereas that of the pTSN-butyrate plasmid used LacIq(ApaI)-F/R primers. The three resulting fragments were assembled using the Gibson Assembly method to obtain the final pSETR-butyrate plasmid. To construct the reporter plasmid, an sgRNA-binding site with an ACG start codon was inserted prior to the second codon of *gfp* in the pREGFP3 plasmid. This was achieved through PCR amplification using the ACG-F and ACG-R primers. The target band was purified using the Wizard SV Gel and PCR Clean-Up System (Promega, Madison, WI, USA). The purified PCR fragment was treated with DpnI and ligated with T4 DNA ligase and T4 polynucleotide kinase. The GFP cassette was PCR-amplified from the resulting plasmid with the pSEVA131-IF and pSEVA131-IR primers, whereas the vector fragment was PCR-amplified from the pSEVA131 plasmid using the pSEVA131-VF and pSEVA131-VR primers. The two fragments were assembled using the Gibson Assembly method to generate pREBE-5C. To create the pSET-sgGFP plasmid, the ts-5C(XhoI)-F and pTet-sg(PacI)-R primers were used for PCR amplification from pRAMBE-sgGFP. The PCR-generated fragment was assembled into the pRAMBE backbone plasmid, which was then treated with XhoI and PacI. To construct plasmids containing the ribozyme variants (Supplementary Table 2), a backbone plasmid was prepared by digesting pSET-sgGFP with XhoI and PacI. The PCR-amplified ribozyme variants created by annealing the DNA oligonucleotides were assembled with the digested pSET-sgGFP plasmid using the Gibson Assembly method. To construct plasmids containing sgRNA variants (Supplementary Table 2), a backbone plasmid was prepared by digesting pRAMBE-sgGFP with XhoI and PacI. The PCR-amplified sgRNA variants created by annealing the DNA oligonucleotides were assembled with the digested pRAMBE-sgGFP plasmid using the Gibson Assembly method. To create the pNR-RAMBE-M plasmid, an engineered ribozyme-sgRNA array was synthesised and amplified using pTet-sg(PstI)-F/pTet-sg(PheA)-R primers and assembled into the pRAMBE backbone treated with PstI-HF/PacI. The accuracy of the constructed plasmid sequences was confirmed using Sanger sequencing (Macrogen).

4.3. Determining the BE efficiency and gene inactivation frequency

EcN and DH5α strains harboring base-editing plasmids were inoculated into 3 mL of LB medium supplemented with 50 μg/mL kanamycin and incubated at 37 °C while shaking at 200 rpm overnight. Subsequently, the cultures were diluted 1:100 (v/v) into 4 mL of fresh LB medium containing 50 μg/mL kanamycin and 250 nM aTc, and incubated under the same conditions. To examine the passage-dependent editing efficiency, cultured cells were diluted every 12 or 24 h at a 1:100 (v/v) ratio in fresh LB medium with identical antibiotic and inducer (aTc) concentrations. To assess C-to-T editing efficiencies at each passage, a 1 μL aliquot of the editing cultures was sampled as a template and amplified via PCR using KOD One PCR Master Mix and site-specific primers (Supplementary Table 3). PCR conditions used are as follows: 10 s at 98 °C, 5 s at 60 °C, and 5 s at 68 °C, for 30 cycles in total. PCR products were confirmed on an agarose gel, purified with the LaboPass Gel and PCR Clean-up Kit, and subjected to Sanger sequencing at Macrogen (Seoul, Republic of Korea). Sequencing chromatograms were visualised using SnapGene (version 4.2.11) and analysed using the online tool EditR (version 1.0.10) [66] to determine the C-to-T base-editing efficiency. Background mutation rates were not subtracted in the calculation of editing efficiencies. Editing efficiencies were directly determined using the EditR program based on the proportion of C-to-T conversions at each target site in the sequencing chromatograms. Unedited control samples were also analyzed, confirming that no significant basal editing occurred under experimental conditions. Next-generation sequencing of PCR products was performed at Celemics (Seoul, Republic of Korea) using Barcode-Tagged Sequencing (BTSeqTM). C-to-T editing efficiency was calculated as the proportion of reads with the desired C-to-T editing in the targeted genomic regions relative to the total sequenced reads. After diluting the edited cultures with sterile phosphate-buffered saline (PBS) and spreading them on LB agar plates, the gene inactivation frequency was determined as the ratio of colonies containing the designed stop codons in the targeted genomic regions to the total number of sequenced colonies.

4.4. Plasmid curing

To acquire plasmid-free strains following genome editing, base-edited cells containing editing plasmids were initially cultured in non-selective LB medium at 37 °C overnight while shaking at 200 rpm. These cultures were subsequently diluted 1:100 (v/v) with fresh LB medium containing 250 nM aTc and incubated for an additional 12 h at 37 °C. Cultures were serially diluted in sterile PBS and plated on non-selective LB agar to isolate individual colonies. From these plates, the absence of editing plasmids in the cells was verified by performing colony PCR and assessing growth in LB medium with and without 50 μg/mL kanamycin.

4.5. Butyrate production

All strains for butyrate production were inoculated into 3 mL of LB medium supplemented with 100 μg/mL ampicillin and incubated overnight at 37 °C with shaking at 200 rpm. The overnight cultures were then diluted 1:100 (v/v) into 5 mL of TB medium containing 100 μg/mL ampicillin and 0.2 mM IPTG. The cultures were subsequently incubated at 37 °C with shaking at 200 rpm for 2 days under micro-aerobic conditions by culturing 5 mL of medium in tightly capped 50 mL Falcon tubes. This setup effectively restricted oxygen transfer while allowing sufficient mixing and nutrient availability. The micro-aerobic cultivation was designed to mimic the limited oxygen environment encountered by EcN in the gastrointestinal tract [67]. Similar micro-aerobic cultivation strategies combined with shaking at 200 rpm have been successfully applied for metabolite production using *E. coli* [68]. Samples were collected at regular intervals for analytical measurements. Following cultivation, cell growth and extracellular metabolites were quantified using spectrophotometry and HPLC, respectively.

4.6. Determination of cell growth and concentrations of extracellular metabolites

To assess cell growth during cultivation, 100-μL cell samples were diluted 1:10 (v/v) with sterile PBS (resulting in a final volume of 1 mL) to measure optical density at a wavelength of 600 nm (OD_{600}) using a UV–VIS spectrophotometer (Ultrospec 8000, GE Healthcare, Uppsala, Sweden). In some experiments, 1 mL aliquots of cells were directly used for growth measurements. To determine glucose, ethanol, and organic acid (D-lactate, succinate, acetate, and butyrate) concentrations in the culture supernatant, bacterial cultures were centrifuged at 3,000 rpm for 20 min at 4 °C to pellet the cells, and 200 μL of the supernatant was filtered through an Advantec 0.45-μm syringe filter. The filtered samples were directly analysed using an HPLC system (Agilent Technologies 1200 series, CA) equipped with a refractive index detector. Typically, 20 μL of each sample was injected and separated on a 1300 × 7.8 mm Aminex HPX-87H column (Bio-Rad, CA, USA) using a mobile phase of 0.4 mM H_2SO_4 (flow rate: 0.5 mL/min). Each analysis had a total runtime of 30 min, with the column temperature maintained at 50 °C. Metabolite concentrations were calculated from standard curves using Microsoft Excel.

4.7. Flow cytometry analysis

All reporter strains were inoculated into 3 mL of LB medium supplemented with 100 μg/mL ampicillin and 50 μg/mL kanamycin and incubated at 37 °C with shaking at 200 rpm overnight. Subsequently, 2 μL of the bacterial culture was added to 198 μL of LB medium containing 100 μg/mL ampicillin, 50 μg/mL kanamycin, and with or without 250 nM aTc in a clear-bottom, black-walled 96-well polystyrene microplate. To prevent evaporation, 200 μL of deionised water was added to the outer moat of the plates. The treated bacteria were then incubated at 37 °C while shaking at 800 rpm on a plate shaker for 12 h. To assess the sfGFP signal, bacterial culture samples were taken, diluted 1:20 with 1 mL of filter-sterilised PBS buffer, and analysed using a FACSCalibur (BD Biosciences) flow cytometer, with the FL1 gain set to 650. The data were analysed using FlowJo software (FlowJo LLC, Ashland, OR, USA). Events were gated based on forward/side scatter (FSC/SSC) to exclude non-cellular events, with at least 10,000 events from the gated cell population recorded at a low flow rate for each experiment. The percentage of GFP-positive cells within the gated population was determined by setting thresholds based on the autofluorescence and FSC/SSC values obtained from the wild-type strain without plasmids, which served as a negative control to define the background fluorescence level. The percentage of GFP-positive cells was calculated as the proportion of the population exhibiting higher fluorescence intensity than this control.

4.8. Statistical analysis

Statistical analyses were conducted using GraphPad Prism 10 software to assess the significance of differences between the two groups. *P*-values were calculated using an unpaired two-tailed *t*-test with Welch's correction, which accounts for unequal variances. Statistical significance is denoted as follows: $*P < 0.05$; $**P < 0.01$; $***P < 0.001$. Non-significant results are indicated as n.s. (not significant) with $P > 0.05$. Specific information regarding the *P*-values can be found in the Source Data File.

CRediT authorship contribution statement

Seung-Gyun Woo: Writing – original draft, Validation, Methodology, Investigation, Formal analysis, Data curation. **Seong Keun Kim:** Writing – original draft, Validation, Resources, Methodology, Formal analysis, Data curation. **Tae Hyun Kim:** Validation, Resources, Formal analysis, Data curation. **Subeen Kim:** Methodology, Formal analysis, Data curation. **Youshin Kim:** Methodology, Formal analysis, Data curation. **Seung-Goo Lee:** Writing – original draft, Investigation, Funding acquisition, Conceptualization. **Dae-Hee Lee:** Writing – review & editing, Writing – original draft, Visualization, Supervision, Project administration, Investigation, Funding acquisition, Data curation, Conceptualization.

Funding

This work was supported by the Bio & Medical Technology Development Program (grant numbers: RS-2018-NR029581, RS-2021-NR056563, RS-2024–00445145, RS-2024–00509115) of the National Research Foundation, funded by the Korean government (MSIT), and by the Korea Research Institute of Bioscience and Biotechnology (KRIBB) Research Initiative Program (KGM1302511). Additional support was provided by the Korea-US Collaborative Research Fund (KUCRF), funded by the Ministry of Science and ICT and the Ministry of Health & Welfare, Republic of Korea (grant number: RS-2024–00468410).

Declaration of competing interest

The authors declare that they have no known competing financial interests or personal relationships that could have appeared to influence the work reported in this paper.

Acknowledgements

The authors thank members of the Synthetic Biology Research Group for their valuable advice. We also appreciate the sharing of the pSEVA plasmids with Dr. Víctor de Lorenzo at the Center for National Biotechnology, CSIC, Madrid, Spain.

Appendix A. Supplementary data

Supplementary data to this article can be found online at https://doi.org/10.1016/j.cej.2025.162336.

Data availability

The data supporting the findings of this work are available within the paper and the Supplementary Information file. All data from the figures can be found in the Source Data File.

References

[1] K.R. Choi, W.D. Jang, D. Yang, J.S. Cho, D. Park, S.Y. Lee, Systems metabolic engineering strategies: Integrating systems and synthetic biology with metabolic engineering, Trends Biotechnol. 37 (8) (2019) 817–837, https://doi.org/10.1016/j.tibtech.2019.01.003.
[2] A. Cubillos-Ruiz, T. Guo, A. Sokolovska, P.F. Miller, J.J. Collins, T.K. Lu, J.M. Lora, Engineering living therapeutics with synthetic biology, Nat. Rev. Drug Discov. 20 (12) (2021) 941–960, https://doi.org/10.1038/s41573-021-00285-3.
[3] A. Rodrigo-Navarro, S. Sankaran, M.J. Dalby, A. del Campo, M. Salmeron-Sanchez, Engineered living biomaterials, Nat. Rev. Mater. 6 (12) (2021) 1175–1190, https://doi.org/10.1038/s41578-021-00350-8.
[4] M.E. Inda, T.K. Lu, Microbes as biosensors, Annu. Rev. Microbiol. 74 (2020) 337–359, https://doi.org/10.1146/annurev-micro-022620-081059.
[5] J.P. Shen, D. Zhao, R. Sasik, J. Luebeck, A. Birmingham, A. Bojorquez-Gomez, K. Licon, K. Klepper, D. Pekin, A.N. Beckett, K.S. Sanchez, A. Thomas, C.C. Kuo, D. Du, A. Roguev, N.E. Lewis, A.N. Chang, J.F. Kreisberg, N. Krogan, L. Qi, T. Ideker, P. Mali, Combinatorial CRISPR-Cas9 screens for de novo mapping of genetic interactions, Nat. Methods 14 (6) (2017) 573–576, https://doi.org/10.1038/nmeth.4225.
[6] D. Kaczmarzyk, I. Cengic, L. Yao, E.P. Hudson, Diversion of the long-chain acyl-ACP pool in *Synechocystis* to fatty alcohols through CRISPRi repression of the essential phosphate acyltransferase PlsX, Metab. Eng. 45 (2018) 59–66, https://doi.org/10.1016/j.ymben.2017.11.014.
[7] F.J. Najm, C. Strand, K.F. Donovan, M. Hegde, K.R. Sanson, E.W. Vaimberg, M. E. Sullender, E. Hartenian, Z. Kalani, N. Fusi, Orthologous CRISPR–Cas9 enzymes for combinatorial genetic screens, Nat. Biotechnol. 36 (2) (2018) 179–189, https://doi.org/10.1038/nbt.4048.
[8] F. Jiang, J.A. Doudna, CRISPR-Cas9 Structures and Mechanisms, Annu Rev Biophys 46 (2017) 505–529, https://doi.org/10.1146/annurev-biophys-062215-010822.
[9] N.S. McCarty, A.E. Graham, L. Studena, R. Ledesma-Amaro, Multiplexed CRISPR technologies for gene editing and transcriptional regulation, Nat Commun 11 (1) (2020) 1281, https://doi.org/10.1038/s41467-020-15053-x.
[10] R. Mans, H.M. van Rossum, M. Wijsman, A. Backx, N.G. Kuijpers, M. van den Broek, P. Daran-Lapujade, J.T. Pronk, A.J. van Maris, J.-M.-G. Daran, CRISPR/Cas9: a molecular Swiss army knife for simultaneous introduction of multiple genetic modifications in *Saccharomyces cerevisiae*, FEMS Yeast Res. 15 (2) (2015) fov004, https://doi.org/10.1093/femsyr/fov004.
[11] T. Jakočiu¯nas, A.S. Rajkumar, J. Zhang, D. Arsovska, A. Rodriguez, C.B. Jendresen, M.L. Skjødt, A.T. Nielsen, I. Borodina, M.K. Jensen, CasEMBLR: Cas9-facilitated multiloci genomic integration of in vivo assembled DNA parts in *Saccharomyces cerevisiae*, ACS Synth. Biol. 4(11) (2015) 1226-1234. https://doi.org/10.1021/acssynbio.5b00007.
[12] W.C. Generoso, M. Gottardi, M. Oreb, E. Boles, Simplified CRISPR-Cas genome editing for *Saccharomyces cerevisiae*, J. Microbiol. Methods 127 (2016) 203–205, https://doi.org/10.1016/j.mimet.2016.06.020.
[13] H.-L. Xing, L. Dong, Z.-P. Wang, H.-Y. Zhang, C.-Y. Han, B. Liu, X.-C. Wang, Q.-J. Chen, A CRISPR/Cas9 toolkit for multiplex genome editing in plants, BMC Plant Biol. 14 (1) (2014) 1–12, https://doi.org/10.1186/s12870-014-0327-y.
[14] X. Ma, Q. Zhang, Q. Zhu, W. Liu, Y. Chen, R. Qiu, B. Wang, Z. Yang, H. Li, Y. Lin, A robust CRISPR/Cas9 system for convenient, high-efficiency multiplex genome editing in monocot and dicot plants, Mol. Plant 8 (8) (2015) 1274–1284, https://doi.org/10.1016/j.molp.2015.04.007.
[15] J. Vad-Nielsen, L. Lin, L. Bolund, A.L. Nielsen, Y. Luo, Golden Gate Assembly of CRISPR gRNA expression array for simultaneously targeting multiple genes, Cell. Mol. Life Sci. 73 (2016) 4315–4325, https://doi.org/10.1007/s00018-016-2271-5.
[16] M. Zuckermann, M. Hlevnjak, H. Yazdanparast, M. Zapatka, D.T. Jones, P. Lichter, J. Gronych, A novel cloning strategy for one-step assembly of multiplex CRISPR

vectors, Sci. Rep. 8 (1) (2018) 17499, https://doi.org/10.1038/s41598-018-35727-3.
[17] C.T. Breunig, T. Durovic, A.M. Neuner, V. Baumann, M.F. Wiesbeck, A. Köferle, M. Götz, J. Ninkovic, S.H. Stricker, One step generation of customizable gRNA vectors for multiplex CRISPR approaches through string assembly gRNA cloning (STAgR), PLoS One 13 (4) (2018) e0196015, https://doi.org/10.1371/journal.pone.0196015.
[18] Y. Zhang, J. Wang, Z. Wang, Y. Zhang, S. Shi, J. Nielsen, Z. Liu, A gRNA-tRNA array for CRISPR-Cas9 based rapid multiplexed genome editing in Saccharomyces cerevisiae, Nat Commun 10 (1) (2019) 1053, https://doi.org/10.1038/s41467-019-09005-3.
[19] Z. Bao, H. Xiao, J. Liang, L. Zhang, X. Xiong, N. Sun, T. Si, H. Zhao, Homology-integrated CRISPR–Cas (HI-CRISPR) system for one-step multigene disruption in *Saccharomyces cerevisiae*, ACS Synth. Biol. 4 (5) (2015) 585–594, https://doi.org/10.1021/sb500255k.
[20] B.F. Cress, O.D. Toparlak, S. Guleria, M. Lebovich, J.T. Stieglitz, J.A. Englaender, J. A. Jones, R.J. Linhardt, M.A. Koffas, CRISPathBrick: modular combinatorial assembly of type II-A CRISPR arrays for dCas9-mediated multiplex transcriptional repression in *E. coli*, ACS Synth. Biol. 4(9) (2015) 987-1000. https://doi.org/10.1021/acssynbio.5b00012.
[21] C. Liao, F. Ttofali, R.A. Slotkowski, S.R. Denny, T.D. Cecil, R.T. Leenay, A.J. Keung, C.L. Beisel, Modular one-pot assembly of CRISPR arrays enables library generation and reveals factors influencing crRNA biogenesis, Nat. Commun. 10 (1) (2019) 2948, https://doi.org/10.1038/s41467-019-10747-3.
[22] B. Zetsche, M. Heidenreich, P. Mohanraju, I. Fedorova, J. Kneppers, E. M. DeGennaro, N. Winblad, S.R. Choudhury, O.O. Abudayyeh, J.S. Gootenberg, Multiplex gene editing by CRISPR–Cpf1 using a single crRNA array, Nat. Biotechnol. 35 (1) (2017) 31–34, https://doi.org/10.1038/nbt.3737.
[23] C.C. Campa, N.R. Weisbach, A.J. Santinha, D. Incarnato, R.J. Platt, Multiplexed genome engineering by Cas12a and CRISPR arrays encoded on single transcripts, Nat. Methods 16 (9) (2019) 887–893, https://doi.org/10.1038/s41592-019-0508-6.
[24] Y. Tong, C.M. Whitford, H.L. Robertsen, K. Blin, T.S. Jorgensen, A.K. Klitgaard, T. Gren, X. Jiang, T. Weber, S.Y. Lee, Highly efficient DSB-free base editing for streptomycetes with CRISPR-BEST, Proc Natl Acad Sci U S A 116 (41) (2019) 20366–20375, https://doi.org/10.1073/pnas.1913493116.
[25] Y. Zhang, Q. Ren, X. Tang, S. Liu, A.A. Malzahn, J. Zhou, J. Wang, D. Yin, C. Pan, M. Yuan, Expanding the scope of plant genome engineering with Cas12a orthologs and highly multiplexable editing systems, Nat. Commun. 12 (1) (2021) 1944, https://doi.org/10.1038/s41467-021-22330-w.
[26] L. Xu, L. Zhao, Y. Gao, J. Xu, R. Han, Empower multiplex cell and tissue-specific CRISPR-mediated gene manipulation with self-cleaving ribozymes and tRNA, Nucleic Acids Res 45 (5) (2017) e28.
[27] M. Kurata, N.K. Wolf, W.S. Lahr, M.T. Weg, M.G. Kluesner, S. Lee, K. Hui, M. Shiraiwa, B.R. Webber, B.S. Moriarity, Highly multiplexed genome engineering using CRISPR/Cas9 gRNA arrays, PLoS One 13 (9) (2018) e0198714, https://doi.org/10.1371/journal.pone.0198714.
[28] R. Ferreira, C. Skrekas, J. Nielsen, F. David, Multiplexed CRISPR/Cas9 genome editing and gene regulation using Csy4 in *Saccharomyces cerevisiae*, ACS Synth. Biol. 7 (1) (2018) 10–15, https://doi.org/10.1021/acssynbio.7b00259.
[29] M. Deaner, J. Mejia, H.S. Alper, Enabling graded and large-scale multiplex of desired genes using a dual-mode dCas9 activator in *Saccharomyces cerevisiae*, ACS Synth. Biol. 6 (10) (2017) 1931–1943, https://doi.org/10.1021/acssynbio.7b00163.
[30] D. Ding, K. Chen, Y. Chen, H. Li, K. Xie, Engineering introns to express RNA guides for Cas9-and Cpf1-mediated multiplex genome editing, Mol. Plant 11 (4) (2018) 542–552, https://doi.org/10.1016/j.molp.2018.02.005.
[31] A.R. Krysler, C.R. Cromwell, T. Tu, J. Jovel, B.P. Hubbard, Guide RNAs containing universal bases enable Cas9/Cas12a recognition of polymorphic sequences, Nat Commun 13 (1) (2022) 1617, https://doi.org/10.1038/s41467-022-29202-x.
[32] S.K. Kim, W. Seong, G.H. Han, D.-H. Lee, S.-G. Lee, CRISPR interference-guided multiplex repression of endogenous competing pathway genes for redirecting metabolic flux in *Escherichia coli*, Microb. Cell Factories 16 (2017) 1–15, https://doi.org/10.1186/s12934-017-0802-x.
[33] A. Hossain, E. Lopez, S.M. Halper, D.P. Cetnar, A.C. Reis, D. Strickland, E. Klavins, H.M. Salis, Automated design of thousands of nonrepetitive parts for engineering stable genetic systems, Nat. Biotechnol. 38 (12) (2020) 1466–1475, https://doi.org/10.1038/s41587-020-0584-2.
[34] J.A. Brophy, C.A. Voigt, Principles of genetic circuit design, Nat. Methods 11 (5) (2014) 508–520, https://doi.org/10.1038/nmeth.2926.
[35] S.C. Sleight, H.M. Sauro, Visualization of evolutionary stability dynamics and competitive fitness of *Escherichia coli* engineered with randomized multigene circuits, ACS Synth. Biol. 2 (9) (2013) 519–528, https://doi.org/10.1021/sb400055h.
[36] T. Ding, C. Huang, Z. Liang, X. Ma, N. Wang, Y.-X. Huo, Reversed paired-gRNA plasmid cloning strategy for efficient genome editing in *Escherichia coli*, Microb. Cell Factories 19 (1) (2020) 1–13, https://doi.org/10.1186/s12934-020-01321-4.
[37] A.C. Reis, S.M. Halper, G.E. Vezeau, D.P. Cetnar, A. Hossain, P.R. Clauer, H. M. Salis, Simultaneous repression of multiple bacterial genes using nonrepetitive extra-long sgRNA arrays, Nat. Biotechnol. 37 (11) (2019) 1294–1301, https://doi.org/10.1038/s41587-019-0286-9.
[38] L. Nissim, S.D. Perli, A. Fridkin, P. Perez-Pinera, T.K. Lu, Multiplexed and programmable regulation of gene networks with an integrated RNA and CRISPR/Cas toolkit in human cells, Mol. Cell 54 (4) (2014) 698–710, https://doi.org/10.1016/j.molcel.2014.04.022.
[39] J. Fredens, K. Wang, D. de la Torre, L.F. Funke, W.E. Robertson, Y. Christova, T. Chia, W.H. Schmied, D.L. Dunkelmann, V. Beránek, Total synthesis of Escherichia coli with a recoded genome, Nature 569 (7757) (2019) 514–518, https://doi.org/10.1038/s41586-019-1192-5.
[40] K. Wang, D. De La Torre, W.E. Robertson, J.W. Chin, Programmed chromosome fission and fusion enable precise large-scale genome rearrangement and assembly, Science 365 (6456) (2019) 922–926, https://doi.org/10.1126/science.aay0737.
[41] A.A. Nielsen, C.A. Voigt, Multi-input CRISPR/C as genetic circuits that interface host regulatory networks, Mol. Syst. Biol. 10 (11) (2014) 763. https://doi.org/10.15252/msb.20145735.
[42] H. Kim, D. Bojar, M. Fussenegger, A CRISPR/Cas9-based central processing unit to program complex logic computation in human cells, Proc. Natl. Acad. Sci. u.s.a. 116 (15) (2019) 7214–7219, https://doi.org/10.1073/pnas.1821740116.
[43] J.P. Lynch, L. Goers, C.F. Lesser, Emerging strategies for engineering Escherichia coli Nissle 1917-based therapeutics, Trends Pharmacol Sci 43 (9) (2022) 772–786, https://doi.org/10.1016/j.tips.2022.02.002.
[44] H. Chen, P. Lei, H. Ji, Q. Yang, B. Peng, J. Ma, Y. Fang, L. Qu, H. Li, W. Wu, L. Jin, D. Sun, Advances in Escherichia coli Nissle 1917 as a customizable drug delivery system for disease treatment and diagnosis strategies, Mater Today Bio 18 (2023) 100543, https://doi.org/10.1016/j.mtbio.2023.100543.
[45] A.J. Triassi, B.D. Fields, C.E. Monahan, J.M. Means, Y. Park, H. Doosthosseini, J.P. Padmakumar, V.M. Isabella, C.A. Voigt, Redesign of an Escherichia coli Nissle treatment for phenylketonuria using insulated genomic landing pads and genetic circuits to reduce burden, Cell Syst 14(6) (2023) 512-524 e12. https://doi.org/10.1016/j.cels.2023.05.004.
[46] A. Casini, F.-Y. Chang, R. Eluere, A.M. King, E.M. Young, Q.M. Dudley, A. Karim, K. Pratt, C. Bristol, A. Forget, A pressure test to make 10 molecules in 90 days: external evaluation of methods to engineer biology, J. Am. Chem. Soc. 140 (12) (2018) 4302–4316, https://doi.org/10.1021/jacs.7b13292.
[47] C. Lou, B. Stanton, Y.J. Chen, B. Munsky, C.A. Voigt, Ribozyme-based insulator parts buffer synthetic circuits from genetic context, Nat Biotechnol 30 (11) (2012) 1137–1142, https://doi.org/10.1038/nbt.2401.
[48] B.K. Cho, K. Zengler, Y. Qiu, Y.S. Park, E.M. Knight, C.L. Barrett, Y. Gao, B. O. Palsson, The transcription unit architecture of the Escherichia coli genome, Nat Biotechnol 27 (11) (2009) 1043–1049, https://doi.org/10.1038/nbt.1582.
[49] T. Zhang, Y. Gao, R. Wang, Y. Zhao, Production of Guide RNAs in vitro and in vivo for CRISPR Using Ribozymes and RNA Polymerase II Promoters, BioProtoc 7 (4) (2017). https://doi.org/10.21769/BioProtoc.2148.
[50] A. Tiyaboonchai, A. Vonada, J. Posey, C. Pelz, L. Wakefield, M. Grompe, Self-cleaving guide RNAs enable pharmacological selection of precise gene editing events in vivo, Nat Commun 13 (1) (2022) 7391, https://doi.org/10.1038/s41467-022-35097-5.
[51] S. Castano-Cerezo, J.M. Pastor, S. Renilla, V. Bernal, J.L. Iborra, M. Canovas, An insight into the role of phosphotransacetylase (pta) and the acetate/acetyl-CoA node in Escherichia coli, Microb Cell Fact 8 (2009) 54, https://doi.org/10.1186/1475-2859-8-54.
[52] E. Tomas-Pejo, C. Gonzalez-Fernandez, S. Greses, C. Kennes, N. Otero-Logilde, M. C. Veiga, D. Bolzonella, B. Muller, V. Passoth, Production of short-chain fatty acids (SCFAs) as chemicals or substrates for microbes to obtain biochemicals, Biotechnol Biofuels Bioprod 16 (1) (2023) 96, https://doi.org/10.1186/s13068-023-02349-5.
[53] R.B. Canani, M.D. Costanzo, L. Leone, M. Pedata, R. Meli, A. Calignano, Potential beneficial effects of butyrate in intestinal and extraintestinal diseases, World J Gastroenterol 17 (12) (2011) 1519–1528, https://doi.org/10.3748/wjg.v17.i12.1519.
[54] D.R. Donohoe, L.B. Collins, A. Wali, R. Bigler, W. Sun, S.J. Bultman, The Warburg effect dictates the mechanism of butyrate-mediated histone acetylation and cell proliferation, Mol Cell 48 (4) (2012) 612–626, https://doi.org/10.1016/j.molcel.2012.08.033.
[55] W. Seong, G.H. Han, H.S. Lim, J.I. Baek, S.-J. Kim, D. Kim, S.K. Kim, H. Lee, H. Kim, S.-G. Lee, Adaptive laboratory evolution of *Escherichia coli* lacking cellular byproduct formation for enhanced acetate utilization through compensatory ATP consumption, Metab. Eng. 62 (2020) 249–259, https://doi.org/10.1016/j.ymben.2020.09.005.
[56] H. Nishimasu, X. Shi, S. Ishiguro, L. Gao, S. Hirano, S. Okazaki, T. Noda, O. O. Abudayyeh, J.S. Gootenberg, H. Mori, Engineered CRISPR-Cas9 nuclease with expanded targeting space, Science 361 (6408) (2018) 1259–1262, https://doi.org/10.1126/science.aas9129.
[57] W.M. Shaw, L. Studena, K. Roy, P. Hapeta, N.S. McCarty, A.E. Graham, T. Ellis, R. Ledesma-Amaro, Inducible expression of large gRNA arrays for multiplexed CRISPRai applications, Nat Commun 13 (1) (2022) 4984, https://doi.org/10.1038/s41467-022-32603-7.
[58] G. Gong, B. Wu, L. Liu, J. Li, Q. Zhu, M. He, G. Hu, Metabolic engineering using acetate as a promising building block for the production of bio-based chemicals, Eng Microbiol 2 (4) (2022) 100036, https://doi.org/10.1016/j.engmic.2022.100036.
[59] K. Novak, S. Pflugl, Towards biobased industry: acetate as a promising feedstock to enhance the potential of microbial cell factories, FEMS Microbiol Lett 365 (20) (2018), https://doi.org/10.1093/femsle/fny226.
[60] A. Krivoruchko, Y. Zhang, V. Siewers, Y. Chen, J. Nielsen, Microbial acetyl-CoA metabolism and metabolic engineering, Metab Eng 28 (2015) 28–42, https://doi.org/10.1016/j.ymben.2014.11.009.
[61] X. Si, W. Shang, Z. Zhou, P. Strappe, B. Wang, A. Bird, C. Blanchard, Gut Microbiome-Induced Shift of Acetate to Butyrate Positively Manages Dysbiosis in High Fat Diet, Mol Nutr Food Res 62 (3) (2018), https://doi.org/10.1002/mnfr.201700670.

[62] S. Facchin, L. Bertin, E. Bonazzi, G. Lorenzon, C. De Barba, B. Barberio, F. Zingone, D. Maniero, M. Scarpa, C. Ruffolo, I. Angriman, E.V. Savarino, Short-Chain Fatty Acids and Human Health: from Metabolic Pathways to Current Therapeutic Implications 14 (2024), https://doi.org/10.3390/life14050559.
[63] R.M. Cooper, J. Hasty, One-Day Construction of Multiplex Arrays to Harness Natural CRISPR-Cas Systems, ACS Synth Biol 9 (5) (2020) 1129–1137, https://doi.org/10.1021/acssynbio.9b00489.
[64] H. Nishimasu, F.A. Ran, P.D. Hsu, S. Konermann, S.I. Shehata, N. Dohmae, R. Ishitani, F. Zhang, O. Nureki, Crystal structure of Cas9 in complex with guide RNA and target DNA, Cell 156 (5) (2014) 935–949, https://doi.org/10.1016/j.cell.2014.02.001.
[65] M.T.A. Nguyen, M.V. Gobry, N. Sampedro Vallina, G. Pothoulakis, E.S. Andersen, Enzymatic Assembly of Small Synthetic Genes with Repetitive Elements, ACS Synth Biol 13(3) (2024) 963-968. https://doi.org/10.1021/acssynbio.3c00665.
[66] M.G. Kluesner, D.A. Nedveck, W.S. Lahr, J.R. Garbe, J.E. Abrahante, B.R. Webber, B.S. Moriarity, EditR: A Method to Quantify Base Editing from Sanger Sequencing, CRISPR J 1 (3) (2018) 239–250, https://doi.org/10.1089/crispr.2018.0014.
[67] X. Yan, X.Y. Liu, D. Zhang, Y.D. Zhang, Z.H. Li, X. Liu, F. Wu, G.Q. Chen, Construction of a sustainable 3-hydroxybutyrate-producing probiotic Escherichia coli for treatment of colitis, Cell Mol Immunol 18 (10) (2021) 2344–2357, https://doi.org/10.1038/s41423-021-00760-2.
[68] L. Zhou, Y. Zhu, Z. Yuan, G. Liu, Z. Sun, S. Du, H. Liu, Y. Li, H. Liu, Z. Zhou, Evaluation of Metabolic Engineering Strategies on 2-Ketoisovalerate Production by Escherichia coli, Appl Environ Microbiol 88 (17) (2022) e0097622, https://doi.org/10.1128/aem.00976-22.